

Testing linearity in semi-functional partially linear regression models

Yongzhen Feng*
Tsinghua University

Jie Li†
Renmin University of China

Xiaojun Song‡
Peking University

Abstract

This paper proposes a Kolmogorov–Smirnov type statistic and a Cramér–von Mises type statistic to test linearity in semi-functional partially linear regression models. Our test statistics are based on a residual marked empirical process indexed by a randomly projected functional covariate, which is able to circumvent the “curse of dimensionality” brought by the functional covariate. The asymptotic properties of the proposed test statistics under the null, the fixed alternative, and a sequence of local alternatives converging to the null at the $n^{1/2}$ rate are established. A straightforward wild bootstrap procedure is suggested to estimate the critical values that are required to carry out the tests in practical applications. Results from an extensive simulation study show that our tests perform reasonably well in finite samples. Finally, we apply our tests to the Tecator and AEMET datasets to check whether the assumption of linearity is supported by these datasets.

Keywords: Functional data; random projections; residual marked empirical process; semi-functional partially linear regression models; wild bootstrap

JEL: C12, C14, C15, C22

*Center for Statistical Science and Department of Industrial Engineering, Tsinghua University, Beijing, 100084, China.

†School of Statistics, Renmin University of China, Beijing, 100872, China. Email: li-jie_stat@ruc.edu.cn.

‡Department of Business Statistics and Econometrics, Guanghua School of Management and Center for Statistical Science, Peking University, Beijing, 100871, China. Email: sxj@gsm.pku.edu.cn.

1 Introduction

Functional Data Analysis (FDA) has gained increasing attention over the last two decades due to the frequently encountered type of data recorded continuously during a time interval or intermittently at several discrete time points, see, e.g., [Ramsay and Silverman \(2005\)](#), [Ferraty and Vieu \(2006\)](#), [Horváth and Kokoszka \(2012\)](#), and more recently [Wang et al. \(2016\)](#), for the development of its theory and applications.

In FDA, an active area of research focuses on the functional linear model (FLM), which assesses the relationship between the functional covariate and other variables via a regression model. The simplest, yet most commonly used model is FLM with a scalar response. A partial list of literature on this topic includes [Yao et al. \(2005\)](#) and [Cai and Hall \(2006\)](#) for estimation and prediction by functional principal component analysis (FPCA) approach, and [Cardot et al. \(2003\)](#) for statistical inference based on hypothesis testing. However, sometimes a single functional covariate is far from enough to explain the response efficiently. Take, for example, the Tecator data set which consists of the fat, water, and protein content of 215 finely chopped meat samples, as well as 215 spectrometric curves measuring the absorbance at 850nm-1050nm wavelength. The goal is to predict the fat content of a meat sample using other variables. If only the spectrometric curve is included as a predictor, the proposed test of [Cuesta-Albertos et al. \(2019\)](#) leads to a rejection of the null of correct specification of FLM, namely, there is no statistically significant evidence that the absorbance curves can sufficiently interpret the fat content.

To address the above issue brought by “mixed data”, which indicates that both a vector of finite length random variables and a function-valued random variable on each individual are of great interest, three main streams of models containing both functional and scalar covariates have been proposed. The first one is a partially functional linear regression model with linearity in both functional and scalar predictors, see, e.g., [Shin \(2009\)](#), [Kong et al. \(2016\)](#) and [Li and Zhu \(2020\)](#). The second kind combines the nonparametric regression for scalar covariates with a standard FLM component, which is called the functional partial linear regression model, see, e.g., [Lian \(2011\)](#). In this paper, we focus our attention on the third type, the semi-functional partially linear regression model (SFPLR), which has the form given as follows:

$$Y = \gamma(Z_1, \dots, Z_p, \mathbf{X}) + \varepsilon = \mathbf{Z}^\top \boldsymbol{\beta} + m(\mathbf{X}) + \varepsilon, \quad (1)$$

where $\mathbf{Z} = (Z_1, \dots, Z_p)^\top$ is a vector of real explanatory variables, \mathbf{X} is another explanatory variable but of functional nature, ε is a random error satisfying $\mathbb{E}(\varepsilon|\mathbf{Z}, \mathbf{X}) = 0$ almost surely (*a.s.*) by construction, $\boldsymbol{\beta} = (\beta_1, \dots, \beta_p)^\top$ is a vector of unknown real parameters and $m(\cdot)$ is an unknown function.

The SFPLR model enjoys wide application since it perfectly captures the flexibility of the nonparametric functional model and the interpretability of standard linear regression. Parameter estimation and its corresponding asymptotic properties in SFPLR have been well developed, see, e.g., [Aneiros-Pérez and Vieu \(2006\)](#), [Aneiros-Perez and Vieu \(2008\)](#), [Boente and Vahnovan \(2017\)](#), and [Aneiros et al. \(2018\)](#), while the goodness-of-fit tests of SFPLR are rather rare in the literature. The term “goodness-of-fit test” was first coined by Pearson for testing if a data distribution belongs to a certain parametric family and has become an important step in model analysis, see, e.g., [Bickel and Rosenblatt \(1973\)](#) and [Durbin \(1973\)](#) for basic ideas and [González-Manteiga and Crujeiras \(2013\)](#) for a comprehensive review. In this paper, the goodness-of-fit goal is to test the linear functional nature of the SFPLR model with the null hypothesis given by

$$H_0 : m(\mathbf{x}) = \langle \mathbf{x}, \boldsymbol{\rho} \rangle \quad \text{for all } \mathbf{x} \in \mathcal{H} \text{ and for some } \boldsymbol{\rho} \in \mathcal{H}, \quad (2)$$

while the alternative hypothesis H_1 is the negation of H_0 , namely, $H_1 : m(\mathbf{x}) \neq \langle \mathbf{x}, \boldsymbol{\rho} \rangle$ for some $\mathbf{x} \in \mathcal{H}$ and for any $\boldsymbol{\rho} \in \mathcal{H}$. Here, \mathcal{H} is a general separable Hilbert space endowed with the inner product $\langle \cdot, \cdot \rangle$, and the functional covariate \mathbf{X} in (1) also takes value in \mathcal{H} . It is noteworthy that testing H_0 against H_1 is quite general within the framework of SFPLR in (1), which includes as a special case testing the significance of functional covariate \mathbf{X} on Y when $\boldsymbol{\rho} = \mathbf{0}$ in (2) and reduces to the goodness-of-fit test for FLM adequacy when $\boldsymbol{\beta} = 0$ in (1).

Testing linearity is of great significance since many datasets in scientific fields are not large enough to guarantee accurate nonparametric estimation and the partially linear models provide feasible and flexible alternatives in the presence of high-dimensional covariates. Usually, some of the covariates are likely to enter the model linearly. In terms of testing the linearity for regression models, the first type focuses on local smoothing-based tests using distances between estimated regression functions under the null and under the alternative, which was employed in [Hardle and Mammen \(1993\)](#), [Fan and Li \(1996\)](#), [Zheng \(1996\)](#) among many others. Another perspective is to consider proper norms of the distance between the estimated integrated regression function and its version under the null, leading to tests based on the residual marked empirical process, see, e.g., [Stute \(1997\)](#) and [Stute et al. \(1998\)](#). However, it is worth noting that the goodness-of-fit tests in the presence of functional covariates are always intricate since the power performance may be greatly deteriorated due to the infinite dimensionality nature of functional data. [Cardot et al. \(2003\)](#), [Delsol et al. \(2011\)](#), and [Hilgert et al. \(2013\)](#) investigated the significance testing of the functional covariate \mathbf{X} on Y from different perspectives. In the context of the FLM goodness-of-fit test, [Patilea et al. \(2012\)](#), enlightened by [Escanciano \(2006\)](#) for the finite-dimensional predictors, put forward the idea of random projections to alleviate the complexity of functional

data and proposed a functional version of the local smoothing-based test to check the linearity in the functional covariate, while [García-Portugués et al. \(2014\)](#) constructed a test based on the projected empirical process taking advantage of the Cramér–von Mises norm without theory. [Cuesta-Albertos et al. \(2019\)](#) successfully derived the weak convergence results by employing the random projection methodology for marked empirical process and utilizing the functional-coefficient estimation proposed in [Cardot et al. \(2007\)](#). However, the testing procedures in all the above works were investigated under the pure FLM and lacked theoretical power analysis for the alternatives. To our best knowledge, there is no literature on goodness-of-fit tests for linearity under the framework of the SFPLR model. Therefore, a practical, computationally efficient, and theoretically reliable testing method is urgently called for to deal with the analysis of the SFPLR model.

In this paper, we employ random projections to test the null hypothesis in order to overcome the well-known “curse of dimensionality” of the functional covariate, which is achieved by considering the inner product of the functional variable \mathbf{X} and a suitable family of projectors $\mathbf{h} \in \mathcal{H}$. Lemma 2.1 of Section 2 indicates that only a finite number of random projections is enough for the characterization of the null hypothesis, making it feasible in practice. To construct tests from the residual marked empirical process based on projections, which are robust to the unknown dependence between the real and functional covariates, a two-step procedure is proposed for parameter estimation. Specifically, one first estimates β under the alternative model, namely, one estimates β under the SFPLR model (1). The reason is that the null model and the alternative model share identical partially linear terms, then the robust estimator $\tilde{\beta}$ obtained from the SFPLR model [see equation (4)] is always consistent irrespective of the model functional form of $m(\mathbf{X})$. After plugging $\tilde{\beta}$ into the model (1), it reduces to a classical FLM and one can easily get the regularized estimate for ρ .

Finally, our test statistics are built via the classical Kolmogorov–Smirnov (KS) and the Cramér–von Mises (CvM) norms adapted to the residual marked empirical process, with the added bonus of $n^{1/2}$ -rate weak convergence as established in Theorem 3.1. Indeed, different from the local smoothing-based tests, our proposed tests are global in nature, with their limiting null distributions enjoying faster convergence rates and free of user-chosen tuning parameters (such as the bandwidths required in the local smoothing-based tests whose proper choice may depend on the underlying data-generating process), and thus our tests are more robust in practical data analysis. In addition, the proposed test statistics are easy to compute and the corresponding critical values can be estimated using a straightforward wild bootstrap procedure. The asymptotic properties of our tests under a fixed alternative hypothesis and a sequence of the local alternative hypotheses converging to the null hypothesis at the $n^{1/2}$ rate are also investigated. To minimize the potential influence of the projection direction \mathbf{h}

and to achieve higher testing power, in the simulations and the real data analysis we suggest choosing $K = 7$ different random directions and then adjust the final p -value by the false discovery rate (FDR) method proposed in [Benjamini and Yekutieli \(2001\)](#). Extensive simulations yield attractive results in terms of empirical sizes and powers that strongly corroborate the asymptotic theory.

The rest of the paper is organized as follows. The testing framework including the hypothesis projection and the two-step estimation procedure is introduced in [Section 2](#). [Section 3](#) presents the asymptotic properties of the proposed test statistics under the null, the alternative, and a sequence of local alternatives. The practical aspects of implementing the tests are given in [Section 4](#), with a detailed discussion of parameter estimation, selection of projection directions, and estimation of critical values through the wild bootstrap procedure. [Section 5](#) reports simulation findings, together with the empirical analysis of the Tecator and AEMET datasets. Finally, [Section 6](#) concludes the paper. All mathematical proofs are collected in the Appendix.

2 Methodology

Throughout this paper, given $\mathbf{h} \in \mathcal{H}$ (\mathbf{h} can be a random element), we denote by $\mathbf{X}^{\mathbf{h}} = \langle \mathbf{X}, \mathbf{h} \rangle$ the projected \mathbf{X} on the direction \mathbf{h} . For any $\mathbf{X} \in \mathcal{H}$, denote its norm by $\|\mathbf{X}\| = \langle \mathbf{X}, \mathbf{X} \rangle^{1/2}$. For any p -dimensional real vector $\mathbf{a} = (a_1, \dots, a_p)^\top \in \mathbb{R}^p$ with $p \geq 1$, denote the Euclidean norm by $\|\mathbf{a}\| = (a_1^2 + \dots + a_p^2)^{1/2}$.

2.1 Hypothesis projection

In this section, we introduce a (mixed) residual marked empirical process indexed by random projections of the functional covariate \mathbf{X} to construct robust specification tests for the linearity of $m(\mathbf{X})$ in the SFPLR model [\(1\)](#). To this end, note that the null hypothesis H_0 in [\(2\)](#) can be equivalently expressed as $H_0 : \mathbb{E}[Y - \mathbf{Z}^\top \boldsymbol{\beta} - \mathbf{X}^\rho | \mathbf{X}] = 0$ *a.s.*, which can also be characterized by means of the associated projected hypothesis on a randomly chosen direction $\mathbf{h} \in \mathcal{H}$, defined as $H_0^{\mathbf{h}} : \mathbb{E}[Y - \mathbf{Z}^\top \boldsymbol{\beta} - \mathbf{X}^\rho | \mathbf{X}^{\mathbf{h}}] = 0$ *a.s.*. For notational simplicity, we denote by $U = Y - \mathbf{Z}^\top \boldsymbol{\beta} - \mathbf{X}^\rho$ in the rest of the article. Note that the error term ε in [\(1\)](#) satisfies $\varepsilon = U$ *a.s.* under the null H_0 . The following important lemma specifies the necessary and sufficient condition such that $\mathbb{E}[U | \mathbf{X}] = 0$ holds *a.s.* based on projections of \mathbf{X} .

Lemma 2.1 (*Theorem 2.4, [Cuesta-Albertos et al. \(2019\)](#)*) *Let μ be a non-degenerate Gaussian measure on \mathcal{H} and \mathbf{X} be a \mathcal{H} -valued random variable (r.v.) defined on a probability space (Ω, σ, ν) . Assume that $m_k := \int \|\mathbf{X}\|^k d\nu < \infty$ for all $k \geq 1$ with $\sum_{k=1}^{\infty} m_k^{-1/k} = \infty$,*

$\mathbb{E} \|\mathbf{Z}\|^2 < \infty$, and $\mathbb{E}[Y^2] < \infty$. Denote $\mathcal{A}_0 := \{\mathbf{h} \in \mathcal{H} : \mathbb{E}[U|\mathbf{X}^{\mathbf{h}}] = 0 \text{ a.s.}\}$, then

$$\mathbb{E}[U|\mathbf{X}] = 0 \quad \text{a.s.} \iff \mu(\mathcal{A}_0) > 0.$$

Remark 2.1 It is obvious that H_0 holds ensures that $H_0^{\mathbf{h}}$ holds for every $\mathbf{h} \in \mathcal{H}$. And the above lemma indicates that if H_0 fails, then $\mu(\mathcal{A}_0) = 0$, implying that with probability one, one can choose a projection \mathbf{h} such that $H_0^{\mathbf{h}}$ fails. Thus we build the μ -a.s. equivalence between the original null hypothesis H_0 and its projected version $H_0^{\mathbf{h}}$.

This enables us to test the null hypothesis H_0 by first randomly choosing a projection direction $\mathbf{h} \in \mathcal{H}$ and then testing the projected null hypothesis conditional on \mathbf{h} , namely $H_0^{\mathbf{h}} : \mathbb{E}[U|\mathbf{X}^{\mathbf{h}}] = 0 \text{ a.s.}$. It is also clear that in $H_0^{\mathbf{h}}$ the conditioning variable $\mathbf{X}^{\mathbf{h}}$ is real, which circumvents the ‘‘curse of dimensionality’’ of functional covariate \mathbf{X} , greatly simplifying the testing problem. Nevertheless, sometimes it is possible that the power of the resulting tests could be sensitive to the selected projection. To minimize the influence of the projection direction and to enhance testing power, we suggest choosing several different directions. A detailed selection procedure on the projection directions is discussed in Section 4.

In light of Lemma 2.1, given $n \geq 1$ independent and identically distributed (i.i.d.) observations $\{Y_i, \mathbf{Z}_i, \mathbf{X}_i\}_{i=1}^n$ with $\mathbf{Z}_i = (Z_{i1}, \dots, Z_{ip})^\top$, we consider the following mixed-type residual marked empirical process built upon the randomly projected functional covariate $\mathbf{X}_i^{\mathbf{h}}$:

$$T_{n,\mathbf{h}}(x) := \frac{1}{\sqrt{n}} \sum_{i=1}^n \mathbb{1}_{\{\mathbf{X}_i^{\mathbf{h}} \leq x\}} \left(Y_i - \mathbf{Z}_i^\top \tilde{\boldsymbol{\beta}} - \mathbf{X}_i^{\hat{\rho}} \right), \quad x \in \mathbb{R}, \quad (3)$$

where the estimator $\tilde{\boldsymbol{\beta}}$ for $\boldsymbol{\beta}$ and the estimator $\hat{\rho}$ for ρ are given in Section 2.2, and $\mathbb{1}_{\{A\}}$ is the indicator function of the event A . To guarantee the consistency of the tests based on $T_{n,\mathbf{h}}(x)$ against all fixed alternatives, it is crucial that $\tilde{\boldsymbol{\beta}}$ should be a robust-type estimator in the sense that it is always consistent regardless of whether the null hypothesis is satisfied. That is, $\tilde{\boldsymbol{\beta}}$ should be obtained under the SFPLR model in (1) rather than under the null model $Y = \mathbf{Z}^\top \boldsymbol{\beta} + \mathbf{X}^\rho + U$ with $U = \varepsilon \text{ a.s.}$, given that \mathbf{Z} and \mathbf{X} may have some unknown dependence structure.

Our test statistics are suitable continuous functionals of $T_{n,\mathbf{h}}(x)$. In this paper, we focus on the popular KS type and CvM type statistics, which are given by

$$\|T_{n,\mathbf{h}}\|_{KS} := \sup_{x \in \mathbb{R}} |T_{n,\mathbf{h}}(x)|$$

and

$$\|T_{n,\mathbf{h}}\|_{CvM} := \int_{\mathbb{R}} T_{n,\mathbf{h}}(x)^2 dF_{n,\mathbf{h}}(x),$$

respectively, where $F_{n,h}(x) = n^{-1} \sum_{i=1}^n \mathbb{1}_{\{\mathbf{X}_i^h \leq x\}}$ is the empirical distribution function (EDF) based on the randomly projected functional covariate $\{\mathbf{X}_i^h\}_{i=1}^n$. The null hypothesis H_0 is rejected whenever the test statistics $\|T_{n,h}\|_{KS}$ and $\|T_{n,h}\|_{CvM}$ exceed some “large” values, which are consistently estimated using a wild bootstrap procedure, as described in Section 4.3.

2.2 Two-step Estimation Procedure

Throughout this paper, denote by \mathcal{H}' the space of continuous linear operators defined in \mathcal{H} and valued in \mathbb{R} . By Riesz’s representation theorem, one can identify the spaces \mathcal{H} and \mathcal{H}' , together with the induced norm of \mathcal{H}' by the following identification condition: for $\mathbf{T} \in \mathcal{H}'$, $\|\mathbf{T}\|_{\mathcal{H}'} = \|\boldsymbol{\tau}\|_{\mathcal{H}}$, where $\boldsymbol{\tau}$ is the unique element in \mathcal{H} such that $\mathbf{T}(x) = \langle \boldsymbol{\tau}, \mathbf{x} \rangle$, $\mathbf{x} \in \mathcal{H}$. For \mathcal{H} -valued continuous linear operator Φ and continuous linear operator Ψ defined in \mathcal{H} , with a slight abuse of notation, define $\Phi\Psi(\mathbf{z}) := \Psi(\Phi(\mathbf{z}))$, $\mathbf{z} \in \mathcal{H}$, representing Ψ composed with Φ .

In order to construct the feasible empirical process $T_{n,h}(x)$ in (3), we first need to obtain an appropriate estimator for $\boldsymbol{\beta}$ in the SFPLR model (1). Note that (1) implies

$$Y - \mathbb{E}(Y|\mathbf{X}) = \sum_{j=1}^p [Z_j - \mathbb{E}(Z_j|\mathbf{X})] \beta_j + \varepsilon.$$

Then, after plugging in the nonparametric estimators for $\mathbb{E}(Y|\mathbf{X})$ and $\{\mathbb{E}(Z_j|\mathbf{X})\}_{j=1}^p$, the resulting least squares type estimator for $\boldsymbol{\beta}$ is given by

$$\tilde{\boldsymbol{\beta}} = \left(\tilde{\mathbf{Z}}_b^\top \tilde{\mathbf{Z}}_b \right)^{-1} \tilde{\mathbf{Z}}_b^\top \tilde{\mathbf{Y}}_b, \quad (4)$$

where the subscript $b = b_n \in \mathbb{R}^+$ represents the bandwidth parameter that converges to zero at some appropriate rate as the sample size n diverges to infinity. In (4), $\tilde{\mathbf{Z}}_b = \mathcal{Z} - \mathbf{W}_b \mathcal{Z} := (\tilde{\mathbf{Z}}_1, \dots, \tilde{\mathbf{Z}}_n)^\top$ and $\tilde{\mathbf{Y}}_b = \mathbf{Y} - \mathbf{W}_b \mathbf{Y} := (\tilde{Y}_1, \dots, \tilde{Y}_n)^\top$, where $\mathcal{Z} = (\mathbf{Z}_1, \dots, \mathbf{Z}_n)^\top$, $\mathbf{Y} = (Y_1, \dots, Y_n)^\top$, and $\mathbf{W}_b = (w_{n,b}(\mathbf{X}_i, \mathbf{X}_j))_{i,j}$ is an $n \times n$ matrix with $w_{n,b}(\cdot, \cdot)$ being the functional covariate version of the Nadaraya–Waston weighting function that has the following form:

$$w_{n,b}(t, \mathbf{X}_i) = \frac{K(d(t, \mathbf{X}_i)/b)}{\sum_{j=1}^n K(d(t, \mathbf{X}_j)/b)},$$

where $K(\cdot)$ is a kernel function from $[0, \infty)$ to $[0, \infty)$, and $d(\cdot, \cdot)$ is a semi-metric in Hilbert space \mathcal{H} . It is noteworthy that $\tilde{\boldsymbol{\beta}}$ in (4) is a robust type estimator for $\boldsymbol{\beta}$ because it is obtained under the unrestricted model (1) and thus is always consistent regardless of whether the null hypothesis holds or not.

Plugging $\tilde{\boldsymbol{\beta}}$ into model (1), under H_0 , the model is transformed into a classical

function linear model

$$\tilde{D} = \mathbf{X}\boldsymbol{\rho} + v,$$

where $\tilde{D} = Y - \mathbf{Z}^\top \tilde{\boldsymbol{\beta}}$ is the generated (i.e., estimated) dependent variable and $v = \varepsilon + \mathbf{Z}^\top (\boldsymbol{\beta} - \tilde{\boldsymbol{\beta}})$ is the composite error term. Finding an estimator for $\boldsymbol{\rho}$ then means seeking the solution to the following minimization problem:

$$\inf_{\boldsymbol{\rho} \in \mathcal{H}} \mathbb{E} \left| \tilde{D} - \mathbf{X}\boldsymbol{\rho} \right|^2.$$

Enlightened by the simple linear regression, $\boldsymbol{\rho}$ is determined by the moment equation $\Delta = \Gamma\boldsymbol{\rho}$, where Δ is the cross-covariance operator of \mathbf{X} and \tilde{D} , defined as $\Delta(\mathbf{z}) := \mathbb{E}[(\mathbf{X} \otimes \tilde{D})(\mathbf{z})]$ for $\mathbf{z} \in \mathcal{H}$ and Γ is the covariance operator of \mathbf{X} given by $\Gamma(\mathbf{z}) := \mathbb{E}[(\mathbf{X} \otimes \mathbf{X})(\mathbf{z})]$ for $\mathbf{z} \in \mathcal{H}$, with \otimes being the Kronecker operator defined as $(\mathbf{x} \otimes \mathbf{y})\mathbf{z} = \langle \mathbf{z}, \mathbf{x} \rangle \mathbf{y}$ for $\mathbf{x}, \mathbf{z} \in \mathcal{H}$ and for \mathbf{y} belonging to either \mathcal{H} or \mathbb{R} .

Obviously, the estimation of $\boldsymbol{\rho}$ needs the reversibility of operator Γ , which is nonnegative, self-adjoint, and nuclear, and thus Hilbert–Schmidt and thus compact. However, due to the infinite-dimensional nature of Hilbert space \mathcal{H} , a bounded inverse of Γ does not exist. The regularization method proposed in [Cardot et al. \(2007\)](#) can effectively tackle this ill-posed issue, for which we first consider the Karhunen–Loève expansion of \mathbf{X} , as given by

$$\mathbf{X} = \sum_{j=1}^{\infty} \lambda_j^{1/2} \xi_j \mathbf{e}_j, \quad (5)$$

where $\{\mathbf{e}_j\}_{j=1}^{\infty}$ is a sequence of orthonormal eigenfunctions of Γ and $\{\xi_j\}_{j=1}^{\infty}$ are centered real r.v.'s such that $\mathbb{E}[\xi_j \xi_{j'}] = \delta_{jj'}$, where $\delta_{jj'}$ is the Kronecker's delta. Assuming the multiplicity of each eigenvalue is one, there then exists a sorted sequence of distinct eigenvalues $\lambda_1 > \lambda_2 > \dots > 0$ of Γ .

To ensure the existence and uniqueness of $\boldsymbol{\rho}$, Assumptions (B1) and (B2) in the next section are required. An empirical finite rank estimator Γ_n^\dagger for Γ^{-1} can be derived by the following procedure:

- (i) Compute the functional principal components (FPC) of $\{\mathbf{X}_i\}_{i=1}^n$, that is, calculate the eigenvalues $\{\hat{\lambda}_j\}$ and eigenfunctions $\{\hat{\mathbf{e}}_j\}$ of Γ_n with $\Gamma_n = n^{-1} \sum_{i=1}^n \mathbf{X}_i \otimes \mathbf{X}_i$;
- (ii) Define a sequence $\{\delta_j\}$, with $\delta_1 := \lambda_1 - \lambda_2$ and $\delta_j := \min(\lambda_j - \lambda_{j+1}, \lambda_{j-1} - \lambda_j)$ for $j \geq 2$, and consider a sequence of thresholds $c_n \in (0, \lambda_1)$, $n \in \mathbb{N}$, with $c_n \rightarrow 0$, then set

$$k_n := \sup \{j \in \mathbb{N} : \lambda_j + \delta_j/2 \geq c_n\}; \quad (6)$$

(iii) Compute Γ_n^\dagger by the following equation:

$$\Gamma_n^\dagger = \sum_{j=1}^{k_n} \frac{1}{\hat{\lambda}_j} \hat{\mathbf{e}}_j \otimes \hat{\mathbf{e}}_j.$$

Observe that Γ_n^\dagger is the population version of Γ^\dagger , which is defined as $\Gamma^\dagger = \sum_{j=1}^{k_n} \lambda_j^{-1} \mathbf{e}_j \otimes \mathbf{e}_j$. Together with the empirical finite rank estimator Δ_n for Δ , denoted by $\Delta_n := n^{-1} \sum_{i=1}^n \mathbf{X}_i \otimes \tilde{D}_i$, the regularized estimator $\hat{\rho}$ for ρ is given by

$$\hat{\rho} := \Gamma_n^\dagger \Delta_n = \frac{1}{n} \sum_{j=1}^{k_n} \sum_{i=1}^n \frac{\langle \mathbf{X}_i \tilde{D}_i, \hat{\mathbf{e}}_j \rangle}{\hat{\lambda}_j} \hat{\mathbf{e}}_j. \quad (7)$$

Having obtained both estimators $\tilde{\beta}$ and $\hat{\rho}$, we can readily compute the residual $\hat{U}_i = Y_i - \mathbf{Z}_i^\top \tilde{\beta} - \mathbf{X}_i \hat{\rho}$ for $i = 1, \dots, n$ to construct the residual marked empirical process $T_{n,h}(x)$ and the test statistics based on it. It is worthwhile to emphasize again that the residual \hat{U}_i is a mixed type (and thus robust) residual in the sense that $\tilde{\beta}$ is obtained under the alternative while $\hat{\rho}$ is obtained under the null. As such, in \hat{U}_i the unknown dependence structure between the real covariate \mathbf{Z} and the functional covariate \mathbf{X} has been taken into account through $\tilde{\beta}$ even if the alternative hypothesis is true. This is in sharp contrast to the standard residual obtained under the null model $Y = \mathbf{Z}^\top \beta + \mathbf{X} \rho + U$, say, $\check{U}_i = Y_i - \mathbf{Z}_i^\top \check{\beta} - \mathbf{X}_i \check{\rho}$ for some $\check{\beta}$ and $\check{\rho}$ obtained when the null holds. Indeed, using the mixed type residual \hat{U}_i in our semiparametric model (1) is very important and guarantees a consistent testing procedure that is robust to the presence of real covariate \mathbf{Z} in (1).

3 Asymptotic properties

3.1 Technical assumptions

To study the asymptotic properties of the proposed test statistics based on $T_{n,h}(x)$ such as $\|T_{n,h}\|_{KS}$ and $\|T_{n,h}\|_{CvM}$ defined in Section 2, we impose the following technical assumptions.

Regularity assumptions

(A1) $m_k := \int \|\mathbf{X}\|^k d\nu < \infty$ for all $k \geq 1$, and $\sum_{k=1}^{\infty} m_k^{-1/k} = \infty$.

(A2) The first and the second moments of ε given \mathbf{X} and \mathbf{Z} are equal to $\mathbb{E}(\varepsilon|\mathbf{X}, \mathbf{Z}) = 0$ *a.s.* and $\mathbb{E}(\varepsilon^2|\mathbf{X}, \mathbf{Z}) = \sigma_\varepsilon^2$ *a.s.*, respectively.

Assumption (A1) is a condition similar to that required in Theorem 3.6 of [Cardot et al. \(2007\)](#) to guarantee the validity of hypothesis projection in Lemma 2.1. Assumption (A2) gives the first two moment constraints of ε given \mathbf{X} and \mathbf{Z} . In particular, the condition $\mathbb{E}(\varepsilon|\mathbf{X}, \mathbf{Z}) = 0$ *a.s.* guarantees that we are testing linearity of the nonparametric functional component within the framework of the SFPLR model in (1). It may be of some interest to test the correct specification of the SFPLR model itself by verifying whether $\mathbb{E}(\varepsilon|\mathbf{X}, \mathbf{Z}) = 0$ *a.s.* holds, which we leave as future research. Although not the weakest, the conditional homoskedasticity is much milder compared with the independence assumption imposed in [Cuesta-Albertos et al. \(2019\)](#).

Assumptions on the estimator $\tilde{\beta}$ in (4)

(B1) $\{\mathbf{X}_i\}_{i=1}^n$ take value in some given compact subset $\mathcal{C} \subset \mathcal{H}$ such that $\mathcal{C} \subset \cup_{k=1}^{\tau_n} \mathcal{B}(x_k, l_n)$, where $\mathcal{B}(x, h) = \{x' \in \mathcal{H} : d(x', x) < h\}$ (with $d(\cdot, \cdot)$ being a semi-metric in \mathcal{H}), x'_k is a series of points in \mathcal{H} , $\tau_n l_n^\gamma = C$, where γ and C are real positive constants and $\tau_n \rightarrow \infty$ and $l_n \rightarrow 0$, as $n \rightarrow \infty$.

(B2) Define $g_j(x) = \mathbb{E}(Z_{ij}|\mathbf{X}_i = x)$ and $\eta_{ij} = Z_{ij} - \mathbb{E}(Z_{ij}|\mathbf{X}_i)$ for $j = 1, \dots, p$, and $\boldsymbol{\eta}_i = (\eta_{i1}, \dots, \eta_{ip})^\top$. For $(u, v) \in \mathcal{C} \times \mathcal{C}$, $f \in \{m, g_1, \dots, g_p\}$, there exist some $C < \infty$ and $\alpha > 0$ such that

$$|f(u) - f(v)| \leq Cd(u, v)^\alpha.$$

There also exists $r \geq 3$ such that $\mathbb{E}|\varepsilon_1|^r + \mathbb{E}|\eta_{11}|^r + \dots + \mathbb{E}|\eta_{1p}|^r < \infty$. In addition, $\mathbf{B} = \mathbb{E}(\boldsymbol{\eta}_1 \boldsymbol{\eta}_1^\top)$ is a $p \times p$ positive definite matrix.

(B3) There exist a positive valued function $\phi(\cdot)$ on $(0, \infty)$ and positive constants α_0, α_1 and α_2 such that

$$\int_0^1 \phi(hs) ds > \alpha_0 \phi(h), \quad \alpha_1 \phi(h) \leq \mathbb{P}(X \in \mathcal{B}(x, h)) \leq \alpha_2 \phi(h), \quad \forall x \in \mathcal{C}, h > 0.$$

(B4) The kernel function $K(\cdot)$ has support $[0, 1]$, is Lipschitz continuous on $[0, \infty]$, and $\exists \theta > 0$ such that $\forall u \in [0, 1], -K'(u) > \theta$. The bandwidth b satisfies that $nb^{4\alpha} \rightarrow 0$ as $n \rightarrow \infty$ and $\phi(b) \geq n^{\frac{2}{r}+d-1}/(\log n)^2$ for n large enough and some constant $d > 0$ satisfying $2/r + d > 1/2$.

Assumptions (B1)-(B4), mainly taken from [Aneiros-Pérez and Vieu \(2006\)](#), allow us to obtain the standard $n^{1/2}$ -rate asymptotic convergence of $\tilde{\beta}$ in (4). The compactness of \mathcal{C} in (B1) and the constraints in (B2) are regular conditions in the setting of nonfunctional partial linear models, see, e.g., [Chen \(1988\)](#), [Bhattacharya and Zhao \(1997\)](#) and [Liang \(2000\)](#), while requirements on τ_n and l_n in (B1) are typical under the framework of

functional nonparametric models, see, e.g., [Ferraty and Vieu \(2006\)](#). (B3) concerns the concentration properties of the small ball probability, which is associated with the semi-metric selection introduced in Chapter 13 of [Ferraty and Vieu \(2006\)](#). The conditions for the kernel function $K(\cdot)$ in (B4) are commonly imposed, while the rates of the bandwidth b in (B4) are required to study the tradeoff between the bias and variance of the estimator $\tilde{\beta}$.

Assumptions on the estimator $\hat{\rho}$ in (7)

(C1) \mathbf{X} , \mathbf{Z} and Y satisfy $\sum_{j=1}^{\infty} \frac{1}{\lambda_j^2} \langle \mathbb{E}(\mathbf{X}W), \mathbf{e}_j \rangle^2 < \infty$, for $W = Y$ or Z_{ij} , $j = 1, 2, \dots, p$.

(C2) The kernel of Γ is $\{\mathbf{0}\}$.

(C3) $\mathbb{E}(\|\mathbf{X}\|^2) < \infty$ and $\mathbb{E}(\|\mathbf{Z}\|^2) < \infty$.

(C4) $\sum_{l=1}^{\infty} |\langle \boldsymbol{\rho}, \mathbf{e}_l \rangle| < \infty$.

(C5) For j large enough, $\lambda_j = \lambda(j)$ with $\lambda(\cdot)$ a convex positive function.

(C6) $\frac{\lambda_n n^4}{\log n} = \mathcal{O}(1)$.

(C7) $\inf \left\{ |\langle \boldsymbol{\rho}, \mathbf{e}_{k_n} \rangle|, \frac{\lambda_{k_n}}{\sqrt{k_n \log k_n}} \right\} = \mathcal{O}(n^{-1/2})$.

(C8) $\sup_j \{\mathbb{E}(|\xi_j|^5)\} \leq M < \infty$ for some $M \geq 1$.

(C9) There exist $C_1, C_2 > 0$ such that $C_1 n^{-1/2} < c_n < C_2 n^{-1/2}$ for every n .

Assumption (C1) ensures the existence of a solution to $\Delta = \Gamma \boldsymbol{\rho}$, and the set of solution is of the form $\boldsymbol{\rho} + \text{Ker}(\Gamma)$, as shown in [Cardot et al. \(2003\)](#). To further simplify the theory development, Assumption (C2) is imposed for identification. Assumptions (C3)-(C8) are standard for the functional linear models, see, e.g., [Cardot et al. \(2007\)](#). In particular, (C5) implies that $\delta_j = \lambda_j - \lambda_{j+1}$ and holds for most classical decreasing rates for eigenvalues, either polynomials or exponential. As such, (C5) is not restrictive. (C6) is analogous to an assumption in Theorem 2 in [Cardot et al. \(2007\)](#). (C7) controls the order of $\langle \mathbf{X}, \mathbf{L}_n \rangle$ [see Lemma A.7 in [Cuesta-Albertos et al. \(2019\)](#)]. It can be easily deduced from (C8) that $\mathbb{E}(\|\mathbf{X}\|^4) < \infty$, which is used to prove Lemma A.3 in the Appendix. (C9) is able to control the behaviour of k_n , as shown by Lemma A.1 in [Cuesta-Albertos et al. \(2019\)](#), entailing that $k_n^3 (\log k_n)^2 = o(n^{1/2})$ together with (C6).

3.2 Asymptotic null distribution

In this section, we establish the asymptotic property of the projected residual marked empirical process $T_{n,h}(x)$ in (3) under H_0^h as well as those of the test statistics based on $T_{n,h}(x)$ such as $\|T_{n,h}\|_{KS}$ and $\|T_{n,h}\|_{CvM}$. First, we introduce two necessary conditions for our theory development.

- (i) $\lim_n t_{n, \mathbb{E}_{x, \mathbf{h}}} < \infty$, where $t_{n, \mathbf{x}} = \sqrt{\sum_{j=1}^{k_n} \lambda_j^{-1} \langle \mathbf{x}, \mathbf{e}_j \rangle^2}$, and $\mathbb{E}_{x, \mathbf{h}} = \mathbb{E} \left(\mathbf{1}_{\{\mathbf{x}_1^{\mathbf{h}} \leq x\}} \mathbf{X}_1 \right)$.
- (ii) $\mathbb{E} [\|\hat{\rho} - \rho\|^4] = \mathcal{O}(n^{-2})$.

The following theorem states that $T_{n, \mathbf{h}}(x)$ converges weakly to a centered Gaussian process with a complicated covariance function under the projected null $H_0^{\mathbf{h}}$.

Theorem 3.1 *Under $H_0^{\mathbf{h}}$, Assumptions (A1)-(A2), (B1)-(B4) and (C1)-(C9), additionally with conditions (i) and (ii), it follows that $T_{n, \mathbf{h}} \xrightarrow{\mathcal{L}} \mathcal{G}$ in $D(\mathbb{R})$, where \mathcal{G} is a centered Gaussian process with covariance function $K(s, t) \equiv C_1(s, t) - C_2(s, t) - C_3(s, t) - C_2(t, s) + C_4(s, t) + C_5(s, t) - C_3(t, s) + C_5(t, s) + C_6(s, t)$, and $D(\mathbb{R})$ is the space of càdlàg functions on \mathbb{R} that are continuous on the right with limit on the left, where*

$$\begin{aligned}
C_1(s, t) &= \int_{\{(\mathbf{x}, \mathbf{z}) : \mathbf{x}^{\mathbf{h}} \leq s \wedge t\}} \text{Var} [Y | \mathbf{X} = \mathbf{x}, \mathbf{Z} = \mathbf{z}] dP_{(\mathbf{X}, \mathbf{Z})}(\mathbf{x}, \mathbf{z}), \\
C_2(s, t) &= \int_{\{(\mathbf{x}, \mathbf{z}) : \mathbf{x}^{\mathbf{h}} \leq s\}} \text{Var} [Y | \mathbf{X} = \mathbf{x}, \mathbf{Z} = \mathbf{z}] \langle \mathbf{E}_{t, \mathbf{h}}, \Gamma^{-1} \mathbf{x} \rangle dP_{(\mathbf{X}, \mathbf{Z})}(\mathbf{x}, \mathbf{z}), \\
C_3(s, t) &= \int_{\{(\mathbf{x}, \mathbf{z}) : \mathbf{x}^{\mathbf{h}} \leq s\}} \text{Var} [Y | \mathbf{X} = \mathbf{x}, \mathbf{Z} = \mathbf{z}] \left(\mathbf{E}_{t, \mathbf{h}}^{\mathbf{Z}} + \mathbf{E}_{t, \mathbf{h}}^{\mathbf{X}, \mathbf{Z}} \right) \mathbf{B}^{-1} \boldsymbol{\eta}_1 dP_{(\mathbf{X}, \mathbf{Z})}(\mathbf{x}, \mathbf{z}), \\
C_4(s, t) &= \int \text{Var} [Y | \mathbf{X} = \mathbf{x}, \mathbf{Z} = \mathbf{z}] \langle \mathbf{E}_{s, \mathbf{h}}, \Gamma^{-1} \mathbf{x} \rangle \langle \mathbf{E}_{t, \mathbf{h}}, \Gamma^{-1} \mathbf{x} \rangle dP_{(\mathbf{X}, \mathbf{Z})}(\mathbf{x}, \mathbf{z}), \\
C_5(s, t) &= \int \text{Var} [Y | \mathbf{X} = \mathbf{x}, \mathbf{Z} = \mathbf{z}] \langle \mathbf{E}_{s, \mathbf{h}}, \Gamma^{-1} \mathbf{x} \rangle \left(\mathbf{E}_{t, \mathbf{h}}^{\mathbf{Z}} + \mathbf{E}_{t, \mathbf{h}}^{\mathbf{X}, \mathbf{Z}} \right) \mathbf{B}^{-1} \boldsymbol{\eta}_1 dP_{(\mathbf{X}, \mathbf{Z})}(\mathbf{x}, \mathbf{z}), \\
C_6(s, t) &= \int \text{Var} [Y | \mathbf{X} = \mathbf{x}, \mathbf{Z} = \mathbf{z}] \left(\mathbf{E}_{s, \mathbf{h}}^{\mathbf{Z}} + \mathbf{E}_{s, \mathbf{h}}^{\mathbf{X}, \mathbf{Z}} \right) \mathbf{B}^{-1} \left(\mathbf{E}_{t, \mathbf{h}}^{\mathbf{Z}} + \mathbf{E}_{t, \mathbf{h}}^{\mathbf{X}, \mathbf{Z}} \right)^{\top} dP_{(\mathbf{X}, \mathbf{Z})}(\mathbf{x}, \mathbf{z}).
\end{aligned}$$

Remark 3.1 *Both conditions (i) and (ii) follow from [Cuesta-Albertos et al. \(2019\)](#). Condition (i) entails that the dominating term of $T_{n, \mathbf{h}}$ in (14) in the Appendix is $T_{n, \mathbf{h}}^1 + T_{n, \mathbf{h}}^3 + T_{n, \mathbf{h}}^5$ and $\|\Gamma^{-1/2} x\| < \infty$, thus ensuring that the covariance function $K(s, t)$ of \mathcal{G} is well-defined. Not as restrictive as it seems to be, condition (ii) can be easily achieved in various practical situations, such as when ρ is a linear combination of a finite number of eigenfunctions of Γ . Moreover, it is only required to obtain the tightness of $T_{n, \mathbf{h}}$.*

Remark 3.2 *It is worth noting that the Gaussian process \mathcal{G} defined in Theorem 3.1 reduces to \mathcal{G}_2 in Theorem 3.3 in [Cuesta-Albertos et al. \(2019\)](#) if one is only interested in testing the linearity of the functional component in the degenerate SFPLR model when $\boldsymbol{\beta} = \mathbf{0}$ is imposed. Our theoretical findings thus include checking the adequacy of the classical FLM as an important special case.*

Remark 3.3 *In general, the dependence between the real covariate \mathbf{Z} and the functional covariate \mathbf{X} cannot be simply ignored. In particular, note that $T_{n, \mathbf{h}}^5$ in (14) represents the estimation uncertainty caused by using $\tilde{\boldsymbol{\beta}}$, the presence of which affects the limiting distribution of the process $T_{n, \mathbf{h}}$. In a very special case, if we assume the mixed-type covariates are*

mutually independent and the response and predictors are all centered, then $T_{n,\mathbf{h}}^5$ in (14) would disappear. Together with Lemma A.2 and Lemma A.8, we can see that for this special case the estimation of the nuisance parameter β plays no role asymptotically in testing linearity under (1). However, since the relation between \mathbf{Z} and \mathbf{X} is usually unknown and non-independent in most practical cases, our paper does complement the existing literature on testing FLM by using a mixed and thus robust type residual to construct our linearity tests in the SFPLR model.

Theorem 3.1 and the continuous mapping theorem then yield the asymptotic null distributions of the continuous functionals of $T_{n,\mathbf{h}}$, including the test statistics $\|T_{n,\mathbf{h}}\|_{KS}$ and $\|T_{n,\mathbf{h}}\|_{CvM}$ based on the KS and CvM norms, respectively.

Corollary 3.1 *Under $H_{0,\mathbf{h}}$, together with Assumptions and conditions in Theorem 3.1, if $\|T_{n,\mathbf{h}}\|_{KS} := \sup_{x \in \mathbb{R}} |T_{n,\mathbf{h}}(x)|$ and $\|T_{n,\mathbf{h}}\|_{CvM} := \int_{\mathbb{R}} T_{n,\mathbf{h}}(x)^2 dF_{\mathbf{h}}(x)$, then*

$$\|T_{n,\mathbf{h}}\|_{KS} \xrightarrow{\mathcal{L}} \|\mathcal{G}\|_{KS} \quad \text{and} \quad \|T_{n,\mathbf{h}}\|_{CvM} \xrightarrow{\mathcal{L}} \int_{\mathbb{R}} \mathcal{G}(x)^2 dF_{\mathbf{h}}(x),$$

where \mathcal{G} is the same Gaussian process as defined in Theorem 3.1, and $F_{\mathbf{h}}(\cdot)$ is the distribution function of $\mathbf{X}^{\mathbf{h}}$.

We reject the null hypothesis whenever $\|T_{n,\mathbf{h}}\|_{KS}$ and $\|T_{n,\mathbf{h}}\|_{CvM}$ exceed some overly “large” values. However, the asymptotic null distributions $\|\mathcal{G}\|_{KS}$ and $\int_{\mathbb{R}} \mathcal{G}(x)^2 dF_{\mathbf{h}}(x)$ in Corollary 3.1 depend on the underlying data-generating process in a highly complicated manner, making a direct application of them infeasible. To implement our KS and CvM tests in practice, in Section 4, we suggest an easy-to-implement wild bootstrap procedure to approximate the critical values of $\|\mathcal{G}\|_{KS}$ and $\int_{\mathbb{R}} \mathcal{G}(x)^2 dF_{\mathbf{h}}(x)$.

3.3 Asymptotic power

Now, we investigate the asymptotic power properties of the KS and CvM tests. We first consider the fixed alternative of the following form:

$$H_1 : \mathbb{E} [\mathbf{Y} - \mathbf{X}^\rho - \mathbf{Z}^\top \beta | \mathbf{X}] \neq 0 \text{ a.s.}, \quad \text{for all } \rho \in \mathcal{H}, \quad (8)$$

with its corresponding projected version

$$H_1^{\mathbf{h}} : \mathbb{E} [\mathbf{Y} - \mathbf{X}^\rho - \mathbf{Z}^\top \beta | \mathbf{X}^{\mathbf{h}}] \neq 0 \text{ a.s.}, \quad \text{for all } \rho \in \mathcal{H}. \quad (9)$$

Note that H_1 and $H_1^{\mathbf{h}}$ are simply the negations of H_0 and $H_0^{\mathbf{h}}$, respectively. The following theorem analyzes the asymptotic property of $T_{n,\mathbf{h}}$ under $H_1^{\mathbf{h}}$.

Theorem 3.2 Under H_1^h , together with Assumptions and conditions in Theorem 3.1, it follows that $n^{-1/2}T_{n,h}(x) \xrightarrow{p} \mathbb{E} \left[(m(\mathbf{X}) - \mathbf{X}^{\rho^*}) \mathbb{1}_{\{\mathbf{X}^h \leq x\}} \right]$ uniformly in $x \in \mathbb{R}$ and for some ρ^* satisfying $\mathbb{E} [\|\hat{\rho} - \rho^*\|] = o(1)$.

Note that ρ^* in Theorem 3.2 should be understood as the probability limit of the two-step estimator $\hat{\rho}$ in \mathcal{H} under H_1^h , i.e., a pseudo true value. As an immediate consequence of Theorem 3.2, under H_1^h such that there exists some x with a positive measure such that $\mathbb{E} \left[(m(\mathbf{X}) - \mathbf{X}^{\rho^*}) \mathbb{1}_{\{\mathbf{X}^h \leq x\}} \right] \neq 0$, the KS statistic $\|T_{n,h}\|_{KS}$ diverges to positive infinity at the rate of $n^{1/2}$, and the CvM statistic $\|T_{n,h}\|_{CvM}$ diverges to positive infinity at the rate of n . This then indicates that our proposed tests are consistent against the fixed projected alternative H_1^h and thus H_1 . Perhaps more interestingly, because of the robust type estimator $\tilde{\beta}$ we used in the mixed residual \hat{U}_i , the consistency of our tests based on $T_{n,h}$ always holds regardless of any (unknown) dependence between the real covariates \mathbf{Z} and the functional covariate \mathbf{X} .

Next, we study the power performance of our tests under a sequence of local alternative hypotheses converging to the null at the parametric rate $n^{-1/2}$ given by:

$$H_{1n} : \mathbb{E} [\mathbf{Y} - \mathbf{X}^\rho - \mathbf{Z}^\top \boldsymbol{\beta} | \mathbf{X}] = n^{-1/2} r(\mathbf{X}), \quad \text{for some } \rho \in \mathcal{H}, \quad (10)$$

with its corresponding projected version

$$H_{1n}^h : \mathbb{E} [\mathbf{Y} - \mathbf{X}^\rho - \mathbf{Z}^\top \boldsymbol{\beta} - n^{-1/2} r(\mathbf{X}) | \mathbf{X}^h] = 0, \quad \text{for some } \rho \in \mathcal{H}, \quad (11)$$

where $r(\cdot)$ is a non-zero function satisfying $\mathbb{E} |r(\mathbf{X})| < \infty$. Note that the function $r(\cdot)$ represents directions of departure from H_0^h , and $n^{-1/2}$ specifies the rate of convergence of H_{1n}^h to H_0^h , the fastest possible rate known in goodness-of-fit testing problems. The following theorem states the asymptotic distribution of $T_{n,h}$ under the sequence of local alternatives H_{1n}^h .

Theorem 3.3 Under H_{1n}^h , together with Assumptions and conditions in Theorem 3.1, it follows that $T_{n,h} \xrightarrow{\mathcal{L}} \mathcal{G} + \Delta$, where \mathcal{G} is the same Gaussian process as defined in Theorem 3.1, and Δ is a deterministic shift function given by $\Delta(x) = \mathbb{E} \left[r(\mathbf{X}) \mathbb{1}_{\{\mathbf{X}^h \leq x\}} \right]$.

Theorem 3.3 and the continuous mapping theorem yield that, under H_{1n}^h ,

$$\|T_{n,h}\|_{KS} \xrightarrow{\mathcal{L}} \|\mathcal{G} + \Delta\|_{KS} \quad \text{and} \quad \|T_{n,h}\|_{CvM} \xrightarrow{\mathcal{L}} \int_{\mathbb{R}} (\mathcal{G}(x) + \Delta(x))^2 dF_h(x).$$

Consequently, our KS and CvM tests have non-negligible asymptotic powers against the sequence of local alternatives H_{1n}^h because the deterministic function $\Delta(x) \neq 0$ for at least some x with a positive measure.

4 Practical Aspects

4.1 Parameter estimation

Estimating the unknown linear coefficients β mainly involves the choice of the semi-metric $d(\cdot, \cdot)$, the kernel function $K(\cdot)$, and the bandwidth b . One has to select among different kinds of semi-metrics which can be drawn by the shape of trajectories of the functional covariate \mathbf{X} . Several approaches, such as Functional PCA semi-metric, partial least-squares (PLS) semi-metric, or derivatives semi-metric are recommended for selecting the semi-metric in [Ferraty and Vieu \(2006\)](#). Throughout our paper, we use the following widely adapted semi-metric:

$$d(\mathcal{X}_i, \mathcal{X}_j) = \left\{ \int (\mathcal{X}_i(t) - \mathcal{X}_j(t))^2 dt \right\}^{1/2}, \quad \mathcal{X}_i, \mathcal{X}_j \in \mathcal{H}.$$

To derive $\tilde{\beta}$ in (4), the quartic kernel $K(u) = 15(1-u^2)^2 \mathbb{I}_{\{|u| \leq 1\}}/16$ is chosen, and the bandwidth has the form $b = cn^{-1/5}$, satisfying Assumption (B4), where c is an adjustment parameter. We have found in extensive simulations that our tests are relatively insensitive to the choice of c . In particular, for the simulations considered, $c = 3$ works quite well and is what we recommended, see Section 5.2.2.

On the other hand, the estimation of the functional coefficient ρ depends on the truncated number k_n . However, it is hard to implement (12) directly since $\{\lambda_j\}$ is usually unknown in practice. As [Cuesta-Albertos et al. \(2019\)](#) suggested, a data-driven way by selecting from a set of candidate k_n 's and choosing the optimal one in terms of a model-selection criterion, such as the Schwartz Information Criterion (SIC), is preferred. To be more specific, denote

$$\text{SIC}(k_n) = \ell(\hat{\rho}_{k_n}) + \frac{\log(n)k_n}{n - k_n - 2}, \quad (12)$$

where $\ell(\hat{\rho}_{k_n})$ represents the log-likelihood of the FLM for ρ estimated with k_n FPC's. The second term $\log(n)k_n/(n - k_n - 2)$ over-penalizes large k_n , which leads to noisy estimates of ρ . Then one can obtain the regularized estimator $\hat{\rho}$ via (7).

4.2 Selection of projection directions

Theoretically speaking, the selection law of projection \mathbf{h} can be arbitrary as long as it has a non-degenerate distribution in \mathcal{H} ; that is, the range of the distribution of the random projection has a positive μ measure. And one only needs to randomly choose one direction. However, in practice, we pay special attention to the selection of projection direction \mathbf{h} in order to guarantee the robustness of the finite-sample performance.

The projection direction \mathbf{h} plays an important role in testing H_0 since it may influence the power of the test significantly. For a special direction that is orthogonal to the data, namely $\mathbf{X}^{\mathbf{h}} = 0$, it will fail to calibrate the level of the test. Since under this projection direction, $T_{n,\mathbf{h}}(x) = n^{-1/2} \sum_{i=1}^n \mathbb{1}_{\{0 \leq x\}} \hat{U}_i$ and $\|T_{n,\mathbf{h}}\|_N = 0$, then the p -value of $H_0^{\mathbf{h}}$ is always 1, which obviously makes no sense. Moreover, different projection directions may yield various outcomes of the test. Both above issues can be tackled by a data-driven approach, which avoids sampling orthogonal directions and allows drawing several directions $\mathbf{h}_1, \dots, \mathbf{h}_K$. After obtaining a number K of different p -values, the final p -value is determined by merging the resulting p -values with the False Discovery Rate (FDR) method in [Benjamini and Yekutieli \(2001\)](#). The detailed procedure is shown in Table 1.

Table 1: A data-driven approach of projection direction selection.

Algorithm 1: Construction of projection directions

Input: Functional covariates $\{\mathbf{X}_i\}_{i=1}^n$

Step 1: Compute the FPC of $\mathbf{X}_1, \dots, \mathbf{X}_n$, namely the eigenpairs $\left\{ \left(\hat{\lambda}_j, \hat{\mathbf{e}}_j \right) \right\}_{j=1}^n$.

Step 2: Choose $j_n := \min \left\{ k = 1, \dots, n-1 : \left(\sum_{j=1}^k \hat{\lambda}_j^2 \right) / \left(\sum_{j=1}^{n-1} \hat{\lambda}_j^2 \right) \leq 0.95 \right\}$.

Step 3: Generate the data-driven projection direction $\mathbf{h} = \sum_{j=1}^{j_n} \eta_j \hat{\mathbf{e}}_j$, with $\eta_j \sim N(0, s_j^2)$, with s_j^2 the sample variance of the scores in the j -th FPC.

Step 4: Repeat Step 3 for K times and then get projection directions $\mathbf{h}_1, \dots, \mathbf{h}_K$.

Output: Projection directions $\mathbf{h}_1, \dots, \mathbf{h}_K$.

4.3 Critical values

As discussed before, the asymptotic null distributions of our test statistics depend on the underlying data-generating process and the corresponding critical values cannot be tabulated. To implement our tests, we use the wild bootstrap method to estimate the critical values in this section. The wild bootstrap procedure is widely adopted in specification testing literature. It particularly works for situations with an unknown form of heteroskedasticity, which is commonly observed in the functional data setting.

To be more precise, the wild bootstrap residual U_i^* for $1 \leq i \leq n$ is defined as $U_i^* = V_i \hat{U}_i$, where $\{V_i\}_{i=1}^n$ is a sequence of i.i.d. random variables with mean zero and variance one and also independent of the original sample $\{Y_i, \mathbf{Z}_i, \mathbf{X}_i\}_{i=1}^n$. One popular choice is $\mathbb{P}(V_i = 1 - \kappa) = \kappa/\sqrt{5}$ and $\mathbb{P}(V_i = \kappa) = 1 - \kappa/\sqrt{5}$ with $\kappa = (\sqrt{5} + 1)/2$, as suggested by [Hardle and Mammen \(1993\)](#). Then, the asymptotic null behavior of $T_{n,\mathbf{h}}(x)$ can be consistently approximated by the following bootstrap process:

$$T_{n,\mathbf{h}}^*(x) = n^{-1/2} \sum_{i=1}^n \left(Y_i^* - \mathbf{Z}_i^\top \tilde{\boldsymbol{\beta}}^* - \mathbf{X}_i \hat{\boldsymbol{\rho}}^* \right) \mathbb{1}_{\{\mathbf{x}_i^{\mathbf{h}} \leq x\}},$$

where $Y_i^* = \mathbf{Z}_i^\top \tilde{\boldsymbol{\beta}} + \mathbf{X}_i^{\hat{\rho}} + U_i^*$ for $1 \leq i \leq n$ is the bootstrap dependent variable, and $\tilde{\boldsymbol{\beta}}^*$ and $\hat{\boldsymbol{\rho}}^*$ are the estimators from the bootstrap sample $\{Y_i^*, \mathbf{Z}_i, \mathbf{X}_i\}_{i=1}^n$. After repeating the above scheme for B times, the p -value is computed by $1/B \sum_{b=1}^B \mathbb{1}\{\|T_{n,\mathbf{h}}\|_N \leq \|T_{n,\mathbf{h}}^{*b}\|_N\}$, with N being either KS or CvM. The next theorem ensures the asymptotic validity of the wild bootstrap procedure.

Theorem 4.1 Under $H_0^{\mathbf{h}}$, together with Assumptions and conditions in Theorem 3.1, for the wild bootstrap process $T_{n,\mathbf{h}}^*$, there exists $T_{n,\mathbf{h}}^* \overset{\mathcal{L}}{\rightsquigarrow} \mathcal{G}^*$ in $D(\mathbb{R})$, where \mathcal{G}^* and \mathcal{G} have the same distribution.

To clarify the whole testing procedure, we give the detailed computational algorithm in the following table.

Algorithm 2: Testing procedure for H_0

Input: Data $\{Y_i, \mathbf{Z}_i, \mathbf{X}_i\}_{i=1}^n$

Step 1. Estimate $\boldsymbol{\beta}$ via (4) with the quadratic kernel and the bandwidth $h = cn^{-1/5}$.

Step 2. Estimate $\boldsymbol{\rho}$ based on (7) for a k_n chosen by (12) and obtain $\hat{U}_i = Y_i - \mathbf{Z}_i^\top \tilde{\boldsymbol{\beta}} - \mathbf{X}_i^{\hat{\rho}}$.

Step 3. Sample several projection directions $\mathbf{h}_1, \dots, \mathbf{h}_K$.

Step 4. For a given \mathbf{h}_i , $i = 1, \dots, K$,

(i) Compute $\|T_{n,\mathbf{h}}\|_N = \left\| n^{-1/2} \sum_{i=1}^n \mathbb{1}_{\{\mathbf{X}_i^{\mathbf{h}} \leq x\}} \hat{U}_i \right\|_N$ with N being either KS or CvM.

(ii) Wild bootstrap resampling. For $b = 1, \dots, B$:

(a) Draw $\{V_i\}_{i=1}^n$, a sequence of i.i.d. random variables such that $\mathbb{P}(V_i = 1 - \kappa) = \kappa/\sqrt{5}$ and $\mathbb{P}(V_i = \kappa) = 1 - \kappa/\sqrt{5}$, where $\kappa = (\sqrt{5} + 1)/2$.

(b) Set $Y_i^* := \mathbf{Z}_i^\top \tilde{\boldsymbol{\beta}} + \mathbf{X}_i^{\hat{\rho}} + U_i^*$ with the bootstrap residual $U_i^* = V_i \hat{U}_i$.

(c) Estimate $\boldsymbol{\beta}^*$ and $\boldsymbol{\rho}^*$ from $\{Y_i^*, \mathbf{Z}_i, \mathbf{X}_i\}_{i=1}^n$ via Step 1 and Step 2.

(d) Obtain the estimated bootstrap residual $\hat{U}_i^* = Y_i^* - \mathbf{Z}_i^\top \tilde{\boldsymbol{\beta}}^* - \mathbf{X}_i^{\hat{\rho}^*}$.

(e) Compute $\|T_{n,\mathbf{h}}^{*b}\|_N = \left\| n^{-1/2} \sum_{i=1}^n \mathbb{1}_{\{\mathbf{X}_i^{\mathbf{h}} \leq x\}} \hat{U}_i^* \right\|_N$.

(iii) Approximate the p -value of $H_0^{\mathbf{h}_i}$ by $p_i = B^{-1} \sum_{b=1}^B \mathbb{1}\{\|T_{n,\mathbf{h}}\|_N \leq \|T_{n,\mathbf{h}}^{*b}\|_N\}$.

Step 5: Set the final p -value of H_0 as $\min_{i=1, \dots, K} \frac{K}{i} p(i)$, where $p(1) \leq \dots \leq p(K)$.

Output: The p -value of H_0 .

5 Simulation study and data application

In this section, we carry out various simulations to illustrate the finite sample performance of our proposed projection-based tests.

5.1 Simulation scenarios

In order to investigate the potential influence of different covariates \mathbf{Z} and \mathbf{X} , as well as the linear coefficient $\boldsymbol{\beta}$ and the functional coefficient $\boldsymbol{\rho}$, we consider 8 possible scenarios. Denote the k -th scenario as Sk , with coefficients $\boldsymbol{\beta}_k$ and $\boldsymbol{\rho}_k$. The deviation from

H_0 is measured by a coefficient δ_d , with $\delta_0 = 0$ corresponding to the null hypothesis, and nonnegative δ_d for $d = 1, 2$, which yield various alternatives. For $H_{k,d}$, the scenario Sk with coefficient δ_d , the data is generated from

$$Y = \mathbf{Z}_k^\top \boldsymbol{\beta}_k + \langle \mathbf{X}, \boldsymbol{\rho}_k \rangle + \delta_d \Delta_{\boldsymbol{\theta}_k}(\mathbf{X}) + \varepsilon, \quad (13)$$

where $\boldsymbol{\theta} = (1, 2, 2, 2, 1, 2, 3, 3)^\top$. The non-linear terms include $\Delta_1(\mathbf{X}) = \|\mathbf{X}\|$, $\Delta_2(\mathbf{X}) = 25 \int_0^1 \int_0^1 \sin(2\pi ts) s(1-s)(1-t) \mathbf{X}(s) \mathbf{X}(t) ds dt$ and $\Delta_3(\mathbf{X}) = \langle e^{-\mathbf{X}}, \mathbf{X}^2 \rangle$. The scalar covariate \mathbf{Z} contains variables $Z_1 \sim N(1, 0.25)$, $Z_2 \sim N(2, 1)$, independent of \mathbf{X} , as well as variables Z_3, Z_4 , which have some certain correlation with \mathbf{X} . The error ε follows the normal distribution $N(0, 0.01)$. The functional process $\mathbf{X}(t)$, centered and valued in $[0, 1]$ with 200 discretized equally spaced points, is as follows:

Brownian Motion (BM): denoted by \mathbf{B} , with eigenfunctions $\psi_j(t) = \sqrt{2} \sin\{(j - 1/2)\pi t\}$, $j \geq 1$.

Functional Process (FP): given by $\mathbf{X}(t) = \sum_{j=1}^{20} \xi_j \phi_j(t)$, where $\phi_j(t) = \sqrt{2} \cos(j\pi t)$ and ξ_j are independent r.v's distributed as $N(0, j^{-2})$.

Brownian Bridge (BB): defined as $\mathbf{X}(t) = \mathbf{B}(t) - t\mathbf{B}(1)$, whose eigenfunctions are $\tilde{\psi}_j(t) = \psi_{j+1/2}(t)$.

Ornstein-Uhlenbeck Process (OU): the Gaussian process with mean function $\mathbb{E}X_t = x_0 e^{-\theta t} + \mu(1 - e^{-\theta t})$ and covariance function $\text{Cov}(\mathbf{X}(s), \mathbf{X}(t)) = \frac{\sigma^2}{2\theta} (e^{-\theta|t-s|} - e^{-\theta(t+s)})$, where $\theta = 1/3$, $\sigma = 1$ and $x_0 = 0$.

Geometric Brownian Motion (GBM): defined as $\mathbf{X}(t) = s_0 \exp\{(\mu - \sigma^2/2)t + \sigma \mathbf{B}(t)\}$, with $\sigma = 1$, $\mu = 1/2$ and $s_0 = 2$.

Table 2 displays the simulation scenarios, including deviations from the null hypothesis. The functional coefficient in S1 and S2 is a finite linear combination of the eigenfunctions of the functional process, with S1 based on Brownian motion and S2 based on Brownian bridge. S3 to S5 consider a finite-dimensional smooth process, and $Z_3 = 10\zeta_3$, $Z_4 = 4\zeta_4$, where ζ_3 and ζ_4 are third and fourth FPC scores of the functional covariate \mathbf{X} , respectively. The functional coefficient is not expressible as a finite combination of eigenfunctions in the next three scenarios: S7 and S8 with the Ornstein-Uhlenbeck processes and S9 with the geometric Brownian motion. The criteria for choosing deviation coefficients δ_d , $d = 1, 2$, in (13) is to add difficulty in distinguishing between the null hypothesis and the alternative. Densities of the response Y under different scenarios are shown in Figure 1, which provides a graphical visualization that all three densities (one under the null and two under the alternative) in every scenario are close, thus making the distinction between the hypotheses tough. Figure 2 exhibits functional curves of \mathbf{X} and the functional coefficients $\boldsymbol{\rho}$, as well as its estimator $\hat{\boldsymbol{\rho}}$ in each scenario. Since S4 and S5 share the same functional covariate and coefficient with S3, thus omitted to save space. Figure 3 exhibits the scaled deviation between the

linear coefficient β and its estimator $\tilde{\beta}$ in each scenario, defined as $\|\beta - \tilde{\beta}\|/\|\beta\|$. One can easily find that the deviation is decreasing with the increase in sample sizes.

Table 2: Summary of the simulated scenarios.

| Scenario | Linear parts $Z^\top \beta$ | Coefficient $\rho(t)$ | Process X | Deviation |
|----------|-----------------------------|---|-----------|---|
| S1 | $2Z_1 + Z_2$ | $(2\psi_1(t) + 4\psi_2(t) + 5\psi_3(t))/\sqrt{2}$ | BM | $\Delta_1, \delta = (0, 2/5, 4/5)^\top$ |
| S2 | $3Z_1 + 2Z_2$ | $(2\tilde{\psi}_1(t) + 4\tilde{\psi}_2(t) + 5\tilde{\psi}_3(t))/\sqrt{2}$ | BB | $\Delta_2, \delta = (0, 5/2, 15/2)^\top$ |
| S3 | $Z_1 + 2Z_2$ | $\sum_{j=1}^{20} 2^{3/2}(-1)^j j^{-2} \phi_j(t)$ | FP | $\Delta_2, \delta = (0, -1, -2)^\top$ |
| S4 | $Z_3 + 2Z_4$ | $\sum_{j=1}^{20} 2^{3/2}(-1)^j j^{-2} \phi_j(t)$ | FP | $\Delta_2, \delta = (0, -1, -3)^\top$ |
| S5 | $2Z_3$ | $\sum_{j=1}^{20} 2^{3/2}(-1)^j j^{-2} \phi_j(t)$ | FP | $\Delta_1, \delta = (0, -1, -2)^\top$ |
| S6 | $2Z_1 + Z_2$ | $\sin(2\pi t) - \cos(2\pi t)$ | OU | $\Delta_2, \delta = (0, -1/4, -1)^\top$ |
| S7 | $2Z_2$ | $t - (t - 3/4)^2$ | OU | $\Delta_3, \delta = (0, -1/100, -1/2)^\top$ |
| S8 | $2Z_1 + Z_2$ | $\pi^2(t^2 - 1/3)$ | GBM | $\Delta_3, \delta = (0, 5/2, 9/2)^\top$ |

5.2 Size and power analysis

5.2.1 Dependence on the number of projections

First, we investigate the adequacy of the tests with respect to the number of projections K , ranging from 1 to 30. To this end, empirical sizes and powers are examined in each scenario with $M = 500$ Monte Carlo experiments and $B = 10000$ bootstrap samples, at level $\alpha = 0.01, 0.05, 0.10$. The sample size n is taken to be 50, 100, and 200, with random projections drawn from the data-driven approach in Table 1. Figure 4 shows the empirical sizes of the CvM and KS tests under the null hypothesis. The empirical rejection rate for each scenario at significance level $\alpha = 0.05$ is displayed in Figure 5. The main findings are summarized as follows:

- (i) **L-shaped patterns in the size curves.** It is clear from Figure 4 that the empirical sizes present apparent decrease as the number K increases, and stabilize below the significance level in each scenario. This is caused by the conservativeness of the FDR method, leading to an increment of the type I error for large K , see [Benjamini and Yekutieli \(2001\)](#).
- (ii) **Occasional bumps yielding power gains.** We can see from Figure 5 that the empirical powers remain constant with large K , and sharp jumps exist at some moderate values of K , providing a significant power gain, especially for the sample size $n = 200$.
- (iii) **Predominance of CvM over KS.** In general, the CvM tests perform much better than the KS tests in power and no worse in size. It is reasonable since quadratic norms in goodness-of-fit are usually more powerful than sup-norms.

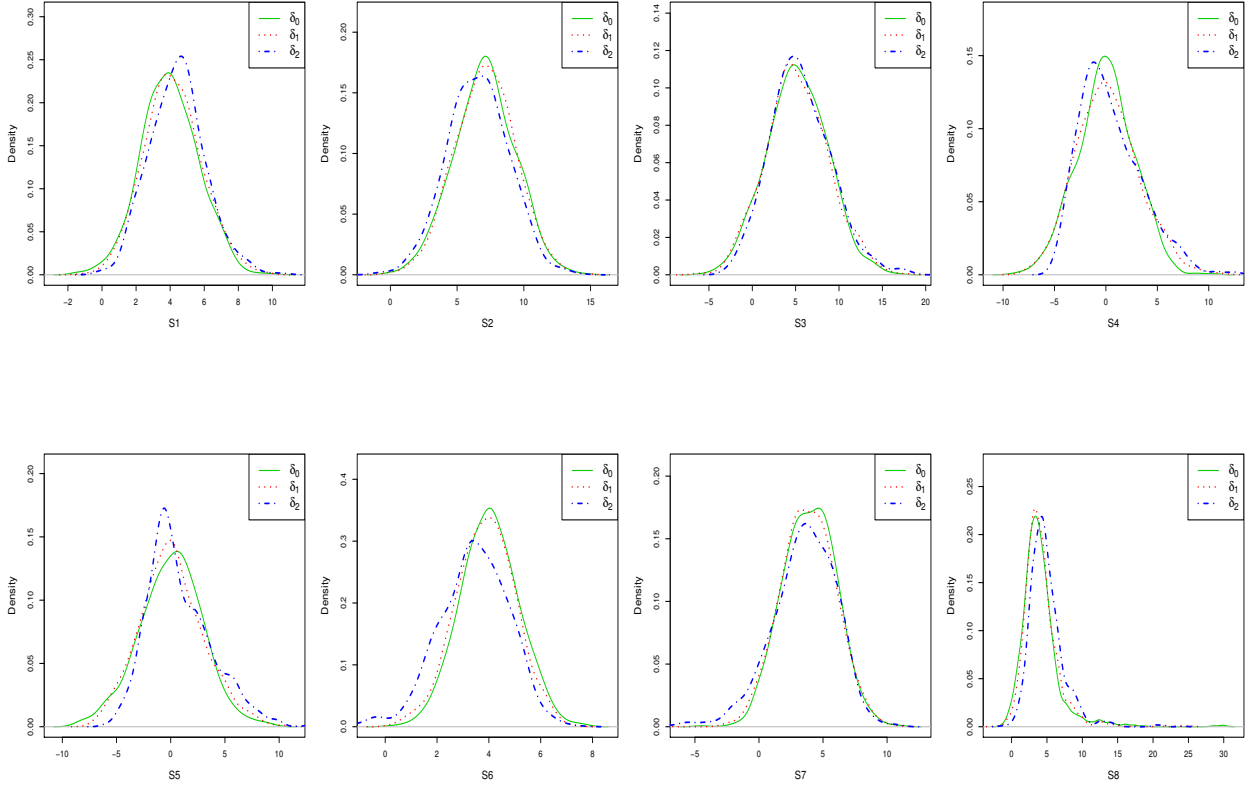


Figure 1: Density plots of the response Y under the null hypothesis $H_{k,0}$ (solid) and two alternatives $H_{k,1}$ (dotted), $H_{k,2}$ (dashed) in scenario S_k , $k = 1, \dots, 8$.

For large K , the tests have an obvious under-rejection of the null hypothesis but a strong power against the alternative. A small K may result in a large size, together with a weak power. Combining these facts, we propose to choose a moderate number $K = 7$, which achieves a perfect balance between the size and power performance. For $n = 200$ and $K = 7$, both CvM and KS tests show accurate calibrations almost in all scenarios based on three significance levels, except $\alpha = 0.10$ for scenarios S2 and S8, and reach a high power either $d = 1$ or $d = 2$. Moreover, the computational ease brought by a not large K is rather important, which avoids a large number of bootstrap times B to maintain the precision, see [Cuesta-Albertos et al. \(2019\)](#).

5.2.2 Dependence on the bandwidth

A bandwidth b is involved in the estimation of the parameter β , then affects the construction of the test. We set the bandwidth $b = cn^{-1/5}$ with c being a tuning constant. In order to explore the influence of c , we check empirical sizes and powers using different bandwidths, with $c = 2, 3, 4$ respectively, based on $M = 500$ Monte Carlo experiments and $B = 10000$ bootstrap samples in each scenario. The results shown in [Table 3](#) imply

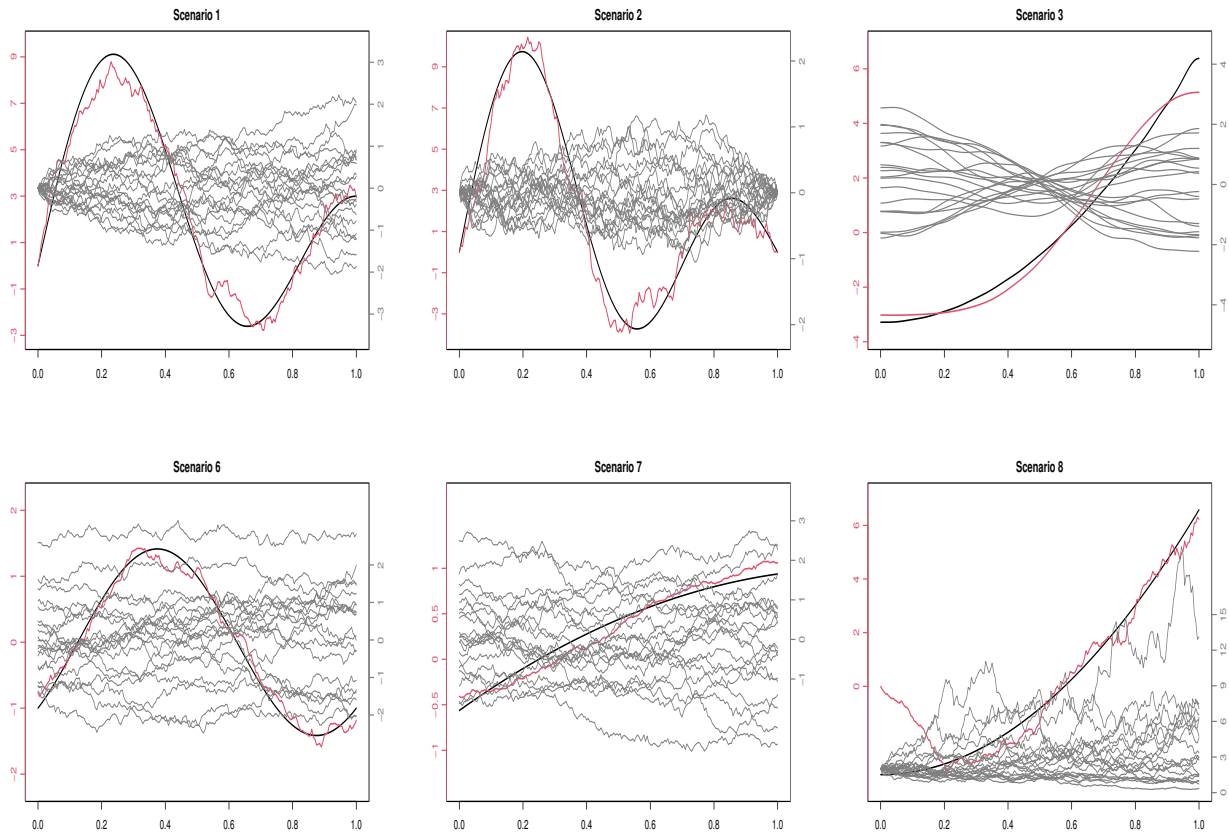


Figure 2: Plots of functional coefficient ρ (black, left scale), its estimate $\hat{\rho}$ (red, left scale) and 20 realizations of the functional covariate \mathbf{X} (grey, right scale) in scenario S_k , $k = 1, 2, 3, 6, 7, 8$.

that the choice of b has little influence either on the size or power of the test since all three bandwidths have decent performance. In most scenarios, the bandwidth with $c = 3$ outperforms the other two in terms of power, except $H_{8,1}$ with $n = 100$. As for empirical sizes, the bandwidth with $c = 2$ and $c = 4$ provide values closer to the pre-determined level for the sample size $n = 50$. As n increases, the size of the bandwidth with $c = 3$ improves dramatically, slightly better than others, especially for $H_{7,0}$ with $n = 200$. In practice, we suggest $c = 3$ as the default value.

Table 4 documents the empirical sizes and powers based on the number of projections $K = 7$ and the bandwidth $b = 3n^{-1/5}$. It is shown that in all scenarios, the level is respected under the null hypothesis, with the approximation being better for a larger sample size. The power is increasing with sample size and tends towards 1 fast as the deviation increases, which reveals a positive confirmation of the effectiveness of the bootstrap correction.

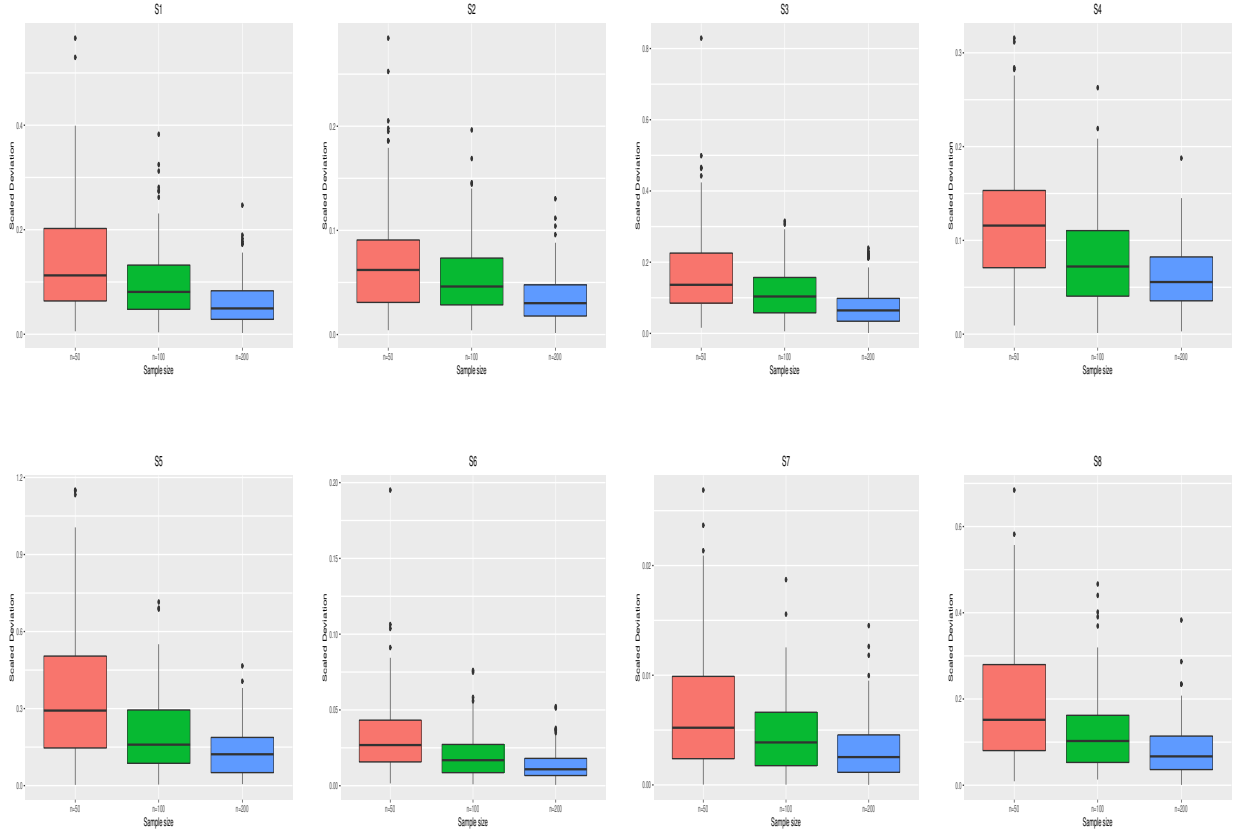


Figure 3: Boxplots of the scaled deviation between the linear coefficient β and its estimator $\hat{\beta}$ in scenario S_k , $k = 1, \dots, 8$.

5.2.3 Power against the local alternatives

Instead of taking a fixed deviation, we let deviation change w.r.t. sample size n for local alternative detection. Scenarios 1, 2, 3, 8 in the previous subsection are considered, with a series of new deviation coefficients $\gamma_n = n^{-1/2}\sqrt{50}\delta_1$, with δ_1 for S1, S2, S3, and S8 being $2/5$, $5/2$, -1 and $5/2$, respectively. For scenario S_k , $k = 1, 2, 3, 8$, the data is generated from

$$Y = \mathbf{Z}_k^\top \beta_k + \langle \mathbf{X}, \rho_k \rangle + \gamma_n \Delta_{\theta_k}(\mathbf{X}) + \varepsilon.$$

Figure 6 gives the empirical power for a Pitman local alternative that departs from the null at a rate of $n^{-1/2}$ at the level $\alpha = 0.05$ with the sample size $n = 50, 100, 200, 300, 500$. We observe that the tests have moderate power, and the power improves or decreases slightly as n increases, but is always large than 0.2, which is consistent with Theorem 3.3.

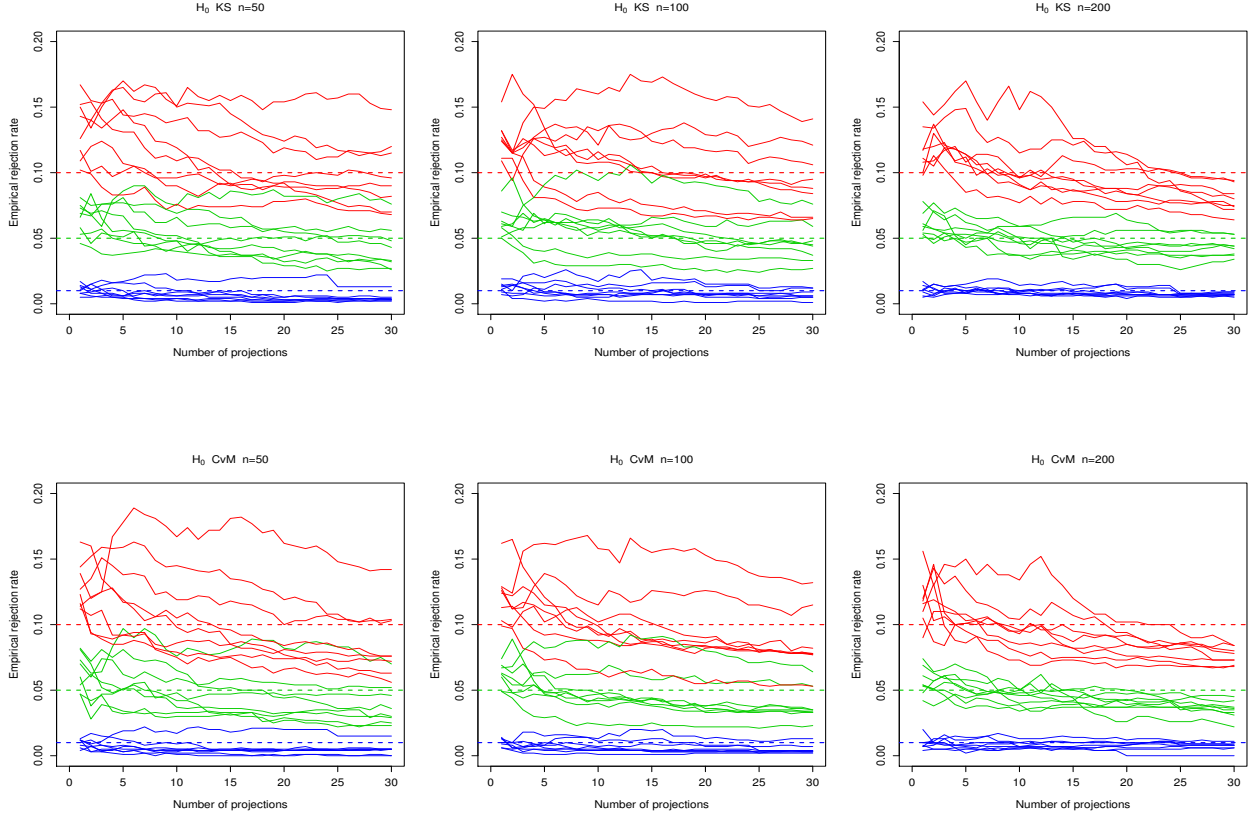


Figure 4: Empirical sizes of the CvM and KS tests with the number of projections from 1 to 30 in scenario S_k , $k = 1, \dots, 8$, based on the sample sizes $n = 50, 100$, and 200 , respectively. The upper, middle, and lower solid lines correspond to the significance levels $\alpha = 0.10, 0.05$, and 0.01 , respectively.

5.3 Real data analysis

The proposed tests are further illustrated with two real data sets containing mixed-type covariates. The first one is the classical Tecator data set with 215 finely chopped pure meat samples, which is available in the R package `fda.usc`. Each sample includes the fat, water, and protein content of the meat, as well as a curve, consisting of 100 channel points of spectrum absorbance in the wavelength range of 850nm-1050nm. These spectra can naturally be regarded as functional data since they are densely recorded at 100 channel points and seem to be quite smooth, see Figure 7 (a). The aim of the study is to predict the fat content Y of a meat sample based on its water content Z_1 , protein content Z_2 and the near-infrared absorbance spectrum \mathbf{X} , hence the SPFLM is chosen as a candidate model. The null hypothesis of interest is:

$$H_0 : Y = \beta_1 Z_1 + \beta_2 Z_2 + \langle \mathbf{X}, \boldsymbol{\rho} \rangle + \varepsilon, \quad \text{for some } \boldsymbol{\rho} \in \mathcal{H}.$$

We apply our proposed method to the above test with $B = 10000$ bootstrap replications. Table 5 presents the p -values at the different numbers of projections. We conclude from the table that the null hypothesis should be retained under the significance level $\alpha = 0.05$. This suggests strongly that there is a significant linear relationship between the fat content and spectrum absorbance curves, contrary to the conclusion in [Cuesta-Albertos et al. \(2019\)](#). The reason is that our goodness-of-fit tests are based on the SFPLR with two added scalar covariates, namely, water and protein content of the meat, while theirs are on the FLM. The difference leads to inverse results, as well as reveals the great value of the test of SPFLR, which is more comprehensive and enjoys broader applications.

The second example is the AEMET data set in the R package `fda.usc`, which consists of a daily temperature of 73 Spanish weather stations during the period 1980-2009 and some other meteorological variables. The right plot of Figure 7 displays the functional observations of the daily temperature. In our study, the goal is to explain the daily wind speed Y (averaged over 1980-2009) through the daily temperature in each weather station (functional covariate \mathbf{X}), and the altitude of each station (scalar covariate Z). The null hypothesis is:

$$H_0 : Y = \beta Z + \langle \mathbf{X}, \boldsymbol{\rho} \rangle + \varepsilon, \quad \text{for some } \boldsymbol{\rho} \in \mathcal{H}.$$

With the same procedures as before, Table 6 reports the p -values at different numbers of projections. Thus we reject the null hypothesis and there is no evidence that the effect of the daily temperature on the wind speed is linear at level $\alpha = 0.05$.

6 Concluding remarks

In our paper, we consider testing functional linearity with the existence of mixed-type covariates in the SFPLR model. A robust two-step parameter estimation procedure is raised in the construction of the test statistics from the projected residual marked empirical process. Theoretical results present that our test statistics converge to a Gaussian process under the null, and are able to detect a series of local alternatives at the parametric rate. The calibration for the critical values of the test statistics is implemented by a wild bootstrap on the residuals. In practice, p -values computed from $K = 7$ random directions are merged with the FDR method to lower the effect of random projection choice.

To complete the goodness-of-fit tests in the presence of both functional covariates and scalar predictors in the future, we list a few potential directions:

(a) Testing functional linearity in semi-functional partial linear quantile regression [[Ding et al. \(2018\)](#)], as a promising extension of our current work.

(b) Testing linearity of scalar covariates in the functional partial linear model [Lian (2011)].

Acknowledgements

This research is supported by the National Natural Science Foundation of China (with grant numbers 71973005, 11771240, and 12026242).

References

- Aneiros, G., Raña, P., Vieu, P., and Vilar, J. (2018). Bootstrap in semi-functional partial linear regression under dependence. *Test*, 27(3):659–679.
- Aneiros-Pérez, G. and Vieu, P. (2006). Semi-functional partial linear regression. *Statistics & Probability Letters*, 76(11):1102–1110.
- Aneiros-Perez, G. and Vieu, P. (2008). Nonparametric time series prediction: A semi-functional partial linear modeling. *Journal of Multivariate Analysis*, 99(5):834–857.
- Benjamini, Y. and Yekutieli, D. (2001). The control of the false discovery rate in multiple testing under dependency. *Annals of statistics*, 29(4):1165–1188.
- Bhattacharya, P. and Zhao, P.-L. (1997). Semiparametric inference in a partial linear model. *Annals of statistics*, 25(1):244–262.
- Bickel, P. J. and Rosenblatt, M. (1973). On some global measures of the deviations of density function estimates. *Annals of Statistics*, 3(6):1071–1095.
- Billingsley, P. (1999). *Convergence of Probability Measures*. Wiley, New York.
- Boente, G. and Vahnovan, A. (2017). Robust estimators in semi-functional partial linear regression models. *Journal of Multivariate Analysis*, 154:59–84.
- Cai, T. T. and Hall, P. (2006). Prediction in functional linear regression. *Annals of Statistics*, 34(5):2159–2179.
- Cardot, H., Ferraty, F., Mas, A., and Sarda, P. (2003). Testing hypotheses in the functional linear model. *Scandinavian Journal of Statistics*, 30(1):241–255.
- Cardot, H., Mas, A., and Sarda, P. (2007). Clt in functional linear regression models. *Probability Theory and Related Fields*, 138(3-4):325–361.
- Chen, H. (1988). Convergence rates for parametric components in a partly linear model. *Annals of Statistics*, 16(1):136–146.
- Cuesta-Albertos, J. A., García-Portugués, E., Febrero-Bande, M., and González-Manteiga, W. (2019). Goodness-of-fit tests for the functional linear model based on randomly projected empirical processes. *Annals of Statistics*, 47(1):439–467.

- Delsol, L., Ferraty, F., and Vieu, P. (2011). Structural test in regression on functional variables. *Journal of Multivariate Analysis*, 102(3):422–447.
- Ding, H., Lu, Z., Zhang, J., and Zhang, R. (2018). Semi-functional partial linear quantile regression. *Statistics & Probability Letters*, 142:92–101.
- Durbin, J. (1973). Weak convergence of the sample distribution function when parameters are estimated. *Annals of Statistics*, 1:279–290.
- Escanciano, J. C. (2006). A consistent diagnostic test for regression models using projections. *Econometric Theory*, 22(6):1030–1051.
- Fan, Y. and Li, Q. (1996). Consistent model specification tests: omitted variables and semiparametric functional forms. *Econometrica*, 64(4):865–890.
- Ferraty, F. and Vieu, P. (2006). *Nonparametric functional data analysis: theory and practice*. Springer Science & Business Media, New York.
- García-Portugués, E., González-Manteiga, W., and Febrero-Bande, M. (2014). A goodness-of-fit test for the functional linear model with scalar response. *Journal of Computational and Graphical Statistics*, 23(3):761–778.
- González-Manteiga, W. and Crujeiras, R. M. (2013). An updated review of goodness-of-fit tests for regression models. *Test*, 22(3):361–411.
- Hardle, W. and Mammen, E. (1993). Comparing nonparametric versus parametric regression fits. *Annals of Statistics*, 21(4):1926–1947.
- Hilgert, N., Mas, A., and Verzelen, N. (2013). Minimax adaptive tests for the functional linear model. *Annals of Statistics*, 41(2):838–869.
- Hoffmann-Jørgensen, J. and Pisier, G. (1976). The law of large numbers and the central limit theorem in banach spaces. *The Annals of Probability*, pages 587–599.
- Horváth, L. and Kokoszka, P. (2012). *Inference for functional data with applications*, volume 200. Springer Science & Business Media, New York.
- Kong, D., Xue, K., Yao, F., and Zhang, H. H. (2016). Partially functional linear regression in high dimensions. *Biometrika*, 103(1):147–159.
- Li, T. and Zhu, Z. (2020). Inference for generalized partial functional linear regression. *Statistica Sinica*, 30(3):1379–1397.
- Lian, H. (2011). Functional partial linear model. *Journal of Nonparametric Statistics*, 23(1):115–128.
- Liang, H. (2000). Asymptotic normality of parametric part in partially linear models with measurement error in the nonparametric part. *Journal of Statistical Planning and Inference*, 86(1):51–62.
- Patilea, V., Sánchez-Sellero, C., and Saumard, M. (2012). Projection-based nonparametric goodness-of-fit testing with functional covariates. *arXiv preprint arXiv:1205.5578*.

- Ramsay, J. O. and Silverman, B. W. (2005). *Functional Data Analysis*. Springer, New York.
- Resnick, S. I. (2014). *Random Variables, Elements, and Measurable Maps*. Springer, New York.
- Shin, H. (2009). Partial functional linear regression. *Journal of Statistical Planning and Inference*, 139(10):3405–3418.
- Stute, W. (1997). Nonparametric model checks for regression. *Annals of Statistics*, 25(2):613–641.
- Stute, W., Thies, S., and Zhu, L.-X. (1998). Model checks for regression: an innovation process approach. *Annals of Statistics*, 26(5):1916–1934.
- Vaart, V. D. and Wellner, J. (1996). *Weak convergence and empirical processes: with applications to statistics*. Springer Science & Business Media, New York.
- Wang, J.-L., Chiou, J.-M., and Müller, H.-G. (2016). Functional data analysis. *Annual Review of Statistics and Its Application*, 3:257–295.
- Yao, F., Müller, H.-G., and Wang, J.-L. (2005). Functional linear regression analysis for longitudinal data. *Annals of Statistics*, 33(6):2873–2903.
- Zheng, J. X. (1996). A consistent test of functional form via nonparametric estimation techniques. *Journal of Econometrics*, 75(2):263–289.

Appendix

A Auxiliary lemmas

We first decompose $T_{n,h}(x)$ into the following five convenient terms:

$$\begin{aligned} T_{n,h}(x) &= n^{-1/2} \sum_{i=1}^n \mathbb{1}_{\{\mathbf{X}_i^h \leq x\}} \left(Y_i - \mathbf{Z}_i^\top \tilde{\boldsymbol{\beta}} - \mathbf{X}_i^{\hat{\boldsymbol{\rho}}} \right) \\ &= n^{-1/2} \left\{ T_{n,h}^1(x) - T_{n,h}^2(x) - T_{n,h}^3(x) - T_{n,h}^4(x) - T_{n,h}^5(x) \right\}, \end{aligned} \quad (14)$$

where

$$\begin{aligned} T_{n,h}^1(x) &:= n^{-1/2} \sum_{i=1}^n \mathbb{1}_{\{\mathbf{X}_i^h \leq x\}} \left(Y_i - \mathbf{Z}_i^\top \boldsymbol{\beta} - \mathbf{X}_i^{\boldsymbol{\rho}} \right), \\ T_{n,h}^2(x) &:= n^{-1/2} \sum_{i=1}^n \left\langle \mathbb{1}_{\{\mathbf{X}_i^h \leq x\}} \mathbf{X}_i - \mathbb{E} \left[\mathbb{1}_{\{\mathbf{X}^h \leq x\}} \mathbf{X} \right], \hat{\boldsymbol{\rho}} - \boldsymbol{\rho} \right\rangle, \\ T_{n,h}^3(x) &:= n^{1/2} \left\langle \mathbb{E} \left[\mathbb{1}_{\{\mathbf{X}^h \leq x\}} \mathbf{X} \right], \hat{\boldsymbol{\rho}} - \boldsymbol{\rho} \right\rangle, \\ T_{n,h}^4(x) &:= n^{-1/2} \sum_{i=1}^n \left(\mathbb{1}_{\{\mathbf{X}_i^h \leq x\}} \mathbf{Z}_i^\top - \mathbb{E} \left[\mathbb{1}_{\{\mathbf{X}^h \leq x\}} \mathbf{Z}_i^\top \right] \right) \left(\tilde{\boldsymbol{\beta}} - \boldsymbol{\beta} \right), \\ T_{n,h}^5(x) &:= n^{1/2} \mathbb{E} \left[\mathbb{1}_{\{\mathbf{X}^h \leq x\}} \mathbf{Z}^\top \right] \left(\tilde{\boldsymbol{\beta}} - \boldsymbol{\beta} \right). \end{aligned}$$

Throughout this section, we employ the following notations for simplicity:

$$\begin{aligned} \bar{\mathbf{X}}_{x,h} &:= \frac{1}{n} \sum_{i=1}^n \mathbb{1}_{\{\mathbf{X}_i^h \leq x\}} \mathbf{X}_i, & \mathbf{E}_{x,h}^{\mathbf{X}} &:= \mathbb{E} \left(\mathbb{1}_{\{\mathbf{X}_1^h \leq x\}} \mathbf{X}_1 \right) = \mathbb{E} \left(\bar{\mathbf{X}}_{x,h} \right), \\ \bar{\mathbf{Z}}_{x,h} &:= \frac{1}{n} \sum_{i=1}^n \mathbb{1}_{\{\mathbf{X}_i^h \leq x\}} \mathbf{Z}_i^T, & \mathbf{E}_{x,h}^{\mathbf{Z}} &:= \mathbb{E} \left(\mathbb{1}_{\{\mathbf{X}_1^h \leq x\}} \mathbf{Z}_1^T \right) = \mathbb{E} \left(\bar{\mathbf{Z}}_{x,h} \right). \end{aligned}$$

We now reproduce two lemmas that are helpful to our proofs.

Lemma A.1 (Theorem 7.5, [Billingsley \(1999\)](#)) Let $(\Omega, \mathcal{F}, \mathbb{P})$ be a probability space and let \mathbf{X} map Ω into $C[0, 1]$. For $F \in C[0, 1]$, denote $\omega(F, h) = \sup_{x, x' \in [0, 1], |x-x'| \leq h} |F(x) - F(x')|$ as the modules of continuity. Suppose that $\mathbf{X}, \mathbf{X}^1, \mathbf{X}^2, \dots$ are random functions. If $(\mathbf{X}_{t_1}^n, \dots, \mathbf{X}_{t_k}^n) \xrightarrow{\mathcal{L}} (\mathbf{X}_{t_1}, \dots, \mathbf{X}_{t_k})$ holds for all t_1, \dots, t_k , and if

$$\lim_{\delta \rightarrow 0} \limsup_{n \rightarrow \infty} \mathbb{P}[\omega(\mathbf{X}^n, \delta) \geq \epsilon] = 0, \quad (15)$$

for each positive ϵ , then $\mathbf{X}^n \xrightarrow{\mathcal{L}} \mathbf{X}$.

Lemma A.2 (Theorem 1, [Aneiros-Pérez and Vieu \(2006\)](#)) Under Assumptions (A2) and

(B1)-(B4),

$$n^{1/2}(\tilde{\boldsymbol{\beta}} - \boldsymbol{\beta}) \overset{\mathcal{L}}{\rightsquigarrow} N(0, \sigma_\varepsilon^2 \mathbf{B}^{-1}). \quad (16)$$

Denote $D_i = Y_i - \mathbf{Z}_i^\top \boldsymbol{\beta}$ and recall $\tilde{D}_i = Y_i - \mathbf{Z}_i^\top \tilde{\boldsymbol{\beta}}$ in Section 2.2, we then decompose $\hat{\boldsymbol{\rho}} - \boldsymbol{\rho}$ into two parts:

$$\hat{\boldsymbol{\rho}} - \boldsymbol{\rho} = (\hat{\boldsymbol{\rho}} - \tilde{\boldsymbol{\rho}}) + (\tilde{\boldsymbol{\rho}} - \boldsymbol{\rho}), \quad (17)$$

where $\tilde{\boldsymbol{\rho}}$ is the estimated functional coefficient based on $\{(\mathbf{X}_i, D_i)\}_{i=1}^n$. Define $\mathbf{U}_n = \frac{1}{n} \sum_{i=1}^n \mathbf{X}_i \otimes \varepsilon_i$ and the definition of $\tilde{\boldsymbol{\rho}}$ leads to

$$\tilde{\boldsymbol{\rho}} = \Gamma_n^\dagger \Gamma_n \boldsymbol{\rho} + (\Gamma_n^\dagger - \Gamma^\dagger) \mathbf{U}_n + \Gamma^\dagger \mathbf{U}_n. \quad (18)$$

Then we derive the following decomposition:

$$\tilde{\boldsymbol{\rho}} - \boldsymbol{\rho} = \mathbf{L}_n + \mathbf{Y}_n + \mathbf{S}_n + \mathbf{R}_n + \mathbf{T}_n, \quad (19)$$

where $\mathbf{L}_n := -\sum_{j=k_n+1}^\infty \langle \boldsymbol{\rho}, \mathbf{e}_j \rangle \mathbf{e}_j$, $\mathbf{Y}_n := \sum_{j=1}^{k_n} (\langle \boldsymbol{\rho}, \hat{\mathbf{e}}_j \rangle \hat{\mathbf{e}}_j - \langle \boldsymbol{\rho}, \mathbf{e}_j \rangle \mathbf{e}_j)$, $\mathbf{S}_n := (\Gamma_n^\dagger - \Gamma^\dagger) \mathbf{U}_n$, $\mathbf{R}_n := \Gamma^\dagger \mathbf{U}_n$, and $\mathbf{T}_n := \Gamma_n^\dagger \Gamma_n \boldsymbol{\rho} - \sum_{j=1}^{k_n} \langle \boldsymbol{\rho}, \hat{\mathbf{e}}_j \rangle \hat{\mathbf{e}}_j$. Note that $\mathbf{T}_n = 0$ by the construction of Γ_n^\dagger .

Equation (20) in [Aneiros-Pérez and Vieu \(2006\)](#) implies that

$$n^{1/2} (\tilde{\boldsymbol{\beta}} - \boldsymbol{\beta}) = \left(n^{-1} \tilde{\mathbf{Z}}_b^\top \tilde{\mathbf{Z}}_b \right)^{-1} n^{-1/2} (S_{n1} - S_{n2} + S_{n3}), \quad (20)$$

where $S_{n1} = \sum_{i=1}^n \tilde{\mathbf{Z}}_i \tilde{m}_b(\mathbf{X}_i)$, $S_{n2} = \sum_{i=1}^n \tilde{\mathbf{Z}}_i (\sum_{l=1}^n w_{n,b}(\mathbf{X}_i, \mathbf{X}_l) \varepsilon_l)$, and $S_{n3} = \sum_{i=1}^n \tilde{\mathbf{Z}}_i \varepsilon_i$. Here, we denote by $\tilde{m}_b(\mathbf{X}_i) = m(\mathbf{X}_i) - \sum_{j=1}^n w_{n,b}(\mathbf{X}_i, \mathbf{X}_j) m(\mathbf{X}_j)$.

Lemma A.3 *Under Assumptions (A2) and (B1)-(B4),*

$$\begin{aligned} n^{-1} \tilde{\mathbf{Z}}_b^\top \tilde{\mathbf{Z}}_b &\overset{a.s.}{\rightarrow} \mathbf{B}, & n^{-1/2} S_{n1} &= o_{a.s.}(1), \\ n^{-1/2} S_{n2} &= o_{a.s.}(1), & n^{-1/2} S_{n3} &= n^{-1/2} \sum_{i=1}^n \boldsymbol{\eta}_i \varepsilon_i + o_{\mathbb{P}}(1). \end{aligned}$$

Proof. See Lemma 7 and proof of Theorem 1 in [Aneiros-Pérez and Vieu \(2006\)](#). ■

In light of (17), the term $T_{n,h}^2(x)$ can be expressed as

$$T_{n,h}^2(x) = n^{1/2} \langle \bar{\mathbf{X}}_{x,h} - \mathbf{E}_{x,h}^{\mathbf{X}}, \hat{\boldsymbol{\rho}} - \tilde{\boldsymbol{\rho}} \rangle + n^{1/2} \langle \bar{\mathbf{X}}_{x,h} - \mathbf{E}_{x,h}^{\mathbf{X}}, \tilde{\boldsymbol{\rho}} - \boldsymbol{\rho} \rangle.$$

The following two lemmas then yield that $T_{n,h}^2(x) = o_{\mathbb{P}}(1)$.

Lemma A.4 Under Assumptions (A2), (C1)-(C6) and (C8)-(C9),

$$n^{1/2} \langle \bar{\mathbf{X}}_{x,h} - \mathbf{E}_{x,h}^{\mathbf{X}}, \tilde{\boldsymbol{\rho}} - \boldsymbol{\rho} \rangle = o_{\mathbb{P}}(1).$$

Proof. See Lemmas A.3 to A.6 in [Cuesta-Albertos et al. \(2019\)](#). ■

Lemma A.5 Under Assumptions (A2), (B2)-(B4) and (C3),

$$n^{1/2} \langle \bar{\mathbf{X}}_{x,h} - \mathbf{E}_{x,h}^{\mathbf{X}}, \hat{\boldsymbol{\rho}} - \tilde{\boldsymbol{\rho}} \rangle = o_{\mathbb{P}}(1).$$

Proof. By construction of the estimator of $\boldsymbol{\rho}$ and Assumption (A2), one has

$$\begin{aligned} \hat{\boldsymbol{\rho}} - \tilde{\boldsymbol{\rho}} &= \Gamma_n^\dagger \left[n^{-1} \sum_{i=1}^n \mathbf{X}_i \otimes (\tilde{D}_i - D_i) \right] \\ &= \Gamma_n^\dagger \left[n^{-1} \sum_{i=1}^n \mathbf{X}_i \otimes \mathbf{Z}_i^\top (\boldsymbol{\beta} - \tilde{\boldsymbol{\beta}}) \right]. \end{aligned}$$

Hence,

$$n^{1/2} \langle \bar{\mathbf{X}}_{x,h} - \mathbf{E}_{x,h}^{\mathbf{X}}, \hat{\boldsymbol{\rho}} - \tilde{\boldsymbol{\rho}} \rangle = \Gamma_n^\dagger \left[n^{-1} \sum_{i=1}^n \langle \mathbf{X}_i, \bar{\mathbf{X}}_{x,h} - \mathbf{E}_{x,h}^{\mathbf{X}} \rangle \mathbf{Z}_i^\top n^{1/2} (\boldsymbol{\beta} - \tilde{\boldsymbol{\beta}}) \right].$$

Note that $\{\mathbf{X}_i\}_{i=1}^n$ are i.i.d. and by the Cauchy–Schwarz inequality,

$$\begin{aligned} \mathbb{E} \left(\langle \mathbf{X}_i, \bar{\mathbf{X}}_{x,h} - \mathbf{E}_{x,h}^{\mathbf{X}} \rangle^2 \right) &= \frac{1}{n^2} \mathbb{E} \left\langle \mathbf{X}_1, \mathbb{1}_{\{\mathbf{X}_1^h \leq x\}} \mathbf{X}_1 - \mathbb{E} \left(\mathbb{1}_{\{\mathbf{X}_1^h \leq x\}} \mathbf{X}_1 \right) \right\rangle^2 \\ &\quad + \frac{n-1}{n^2} \mathbb{E} \left\langle \mathbf{X}_2, \mathbb{1}_{\{\mathbf{X}_1^h \leq x\}} \mathbf{X}_1 - \mathbb{E} \left(\mathbb{1}_{\{\mathbf{X}_1^h \leq x\}} \mathbf{X}_1 \right) \right\rangle^2 \\ &= \frac{1}{n^2} \mathbb{E} \left[\left\langle \mathbf{X}_1, \mathbb{1}_{\{\mathbf{X}_1^h \leq x\}} \mathbf{X}_1 \right\rangle - \left\langle \mathbf{X}_1, \mathbb{E} \left(\mathbb{1}_{\{\mathbf{X}_1^h \leq x\}} \mathbf{X}_1 \right) \right\rangle \right]^2 \\ &\quad + \frac{n-1}{n^2} \mathbb{E} \left[\left\langle \mathbf{X}_2, \mathbb{1}_{\{\mathbf{X}_1^h \leq x\}} \mathbf{X}_1 \right\rangle - \left\langle \mathbf{X}_2, \mathbb{E} \left(\mathbb{1}_{\{\mathbf{X}_1^h \leq x\}} \mathbf{X}_1 \right) \right\rangle \right]^2 \\ &\leq \frac{2}{n^2} \left[\mathbb{E} \left\langle \mathbf{X}_1, \mathbb{1}_{\{\mathbf{X}_1^h \leq x\}} \mathbf{X}_1 \right\rangle^2 + \mathbb{E} \left\langle \mathbf{X}_1, \mathbb{E} \left(\mathbb{1}_{\{\mathbf{X}_1^h \leq x\}} \mathbf{X}_1 \right) \right\rangle^2 \right] \\ &\quad + \frac{2n-2}{n^2} \left[\mathbb{E} \left\langle \mathbf{X}_2, \mathbb{1}_{\{\mathbf{X}_1^h \leq x\}} \mathbf{X}_1 \right\rangle^2 + \mathbb{E} \left\langle \mathbf{X}_2, \mathbb{E} \left(\mathbb{1}_{\{\mathbf{X}_1^h \leq x\}} \mathbf{X}_1 \right) \right\rangle^2 \right] \\ &\leq \frac{2}{n^2} \left[\mathbb{E} \|\mathbf{X}_1\|^2 \mathbb{E} \left\| \mathbb{1}_{\{\mathbf{X}_1^h \leq x\}} \mathbf{X}_1 \right\|^2 + \mathbb{E} \|\mathbf{X}_1\|^2 \mathbb{E} \left\| \mathbb{1}_{\{\mathbf{X}_1^h \leq x\}} \mathbf{X}_1 \right\|^2 \right] \\ &\quad + \frac{2n-2}{n^2} \left[\mathbb{E} \|\mathbf{X}_2\|^2 \mathbb{E} \left\| \mathbb{1}_{\{\mathbf{X}_1^h \leq x\}} \mathbf{X}_1 \right\|^2 + \mathbb{E} \|\mathbf{X}_2\|^2 \mathbb{E} \left\| \mathbb{1}_{\{\mathbf{X}_1^h \leq x\}} \mathbf{X}_1 \right\|^2 \right] \\ &\leq \frac{2}{n^2} \mathbb{E} \|\mathbf{X}_1\|^4 + \frac{4n-2}{n^2} (\mathbb{E} \|\mathbf{X}_1\|^2)^2. \end{aligned}$$

Thus,

$$\begin{aligned} & \mathbb{E} \left| n^{-1} \sum_{i=1}^n \langle \mathbf{X}_i, \bar{\mathbf{X}}_{x,h} - \mathbf{E}_{x,h}^{\mathbf{X}} \rangle \mathbf{Z}_i^\top \right| \leq \mathbb{E} \left| \langle \mathbf{X}_1, \bar{\mathbf{X}}_{x,h} - \mathbf{E}_{x,h}^{\mathbf{X}} \rangle \mathbf{Z}_1^\top \right| \\ & \leq \mathbb{E} \left(\langle \mathbf{X}_1, \bar{\mathbf{X}}_{x,h} - \mathbf{E}_{x,h}^{\mathbf{X}} \rangle^2 \right) \mathbb{E} \|\mathbf{Z}_1^\top\|^2 \leq \left\{ \frac{2}{n^2} \mathbb{E} \|\mathbf{X}_1\|^4 + \frac{4n-2}{n^2} \{ \mathbb{E} \|\mathbf{X}_1\|^2 \}^2 \right\} \mathbb{E} \|\mathbf{Z}_1^\top\|^2. \end{aligned}$$

Together with Assumption (C3), one concludes that $n^{-1} \sum_{i=1}^n \langle \mathbf{X}_i, \bar{\mathbf{X}}_{x,h} - \mathbf{E}_{x,h}^{\mathbf{X}} \rangle \mathbf{Z}_i^\top = o_{\mathbb{P}}(1)$. Combining with Lemma A.2, it follows that

$$n^{-1} \sum_{i=1}^n \langle \mathbf{X}_i, \bar{\mathbf{X}}_{x,h} - \mathbf{E}_{x,h}^{\mathbf{X}} \rangle \mathbf{Z}_i^\top n^{1/2} (\boldsymbol{\beta} - \tilde{\boldsymbol{\beta}}) = o_{\mathbb{P}}(1).$$

In addition, since Γ_n^\dagger is a finite-rank operator, it is compact. Thus, the proof is completed by Theorem 6.3.1 in Resnick (2014). ■

Lemma A.6 Under Assumptions (C3), (C4), (C6) and (C7), one has

$$n^{1/2} \langle \mathbf{E}_{x,h}^{\mathbf{X}}, \tilde{\boldsymbol{\rho}} - \boldsymbol{\rho} \rangle = n^{-1/2} \sum_{i=1}^n \langle \mathbf{E}_{x,h}^{\mathbf{X}}, \Gamma^\dagger \mathbf{X}_i \rangle \varepsilon_i + o_{\mathbb{P}}(1).$$

Proof. See the proof of Lemma A.7 in Cuesta-Albertos et al. (2019). ■

Lemma A.7 Under condition (i), Assumptions (A2), (B1)-(B4), (C3) and (C9),

$$n^{1/2} \langle \mathbf{E}_{x,h}^{\mathbf{X}}, \hat{\boldsymbol{\rho}} - \tilde{\boldsymbol{\rho}} \rangle = \mathbf{E}_{x,h}^{\mathbf{X},\mathbf{Z}} \mathbf{B}^{-1} n^{-1/2} \sum_{i=1}^n \boldsymbol{\eta}_i \varepsilon_i + o_{\mathbb{P}}(1),$$

with $\mathbf{E}_{x,h}^{\mathbf{X},\mathbf{Z}}$ defined as $-\mathbb{E} [\langle \Gamma^{-1} \mathbf{X}, \mathbf{E}_{x,h}^{\mathbf{X}} \rangle \mathbf{Z}^\top]$.

Proof. Similar to the proof of Lemma A.5, by replacing $(\bar{\mathbf{X}}_{x,h} - \mathbf{E}_{x,h}^{\mathbf{X}})$ with $\mathbf{E}_{x,h}^{\mathbf{X}}$, one obtains

$$\begin{aligned} \langle n^{1/2} \mathbf{E}_{x,h}^{\mathbf{X}}, \hat{\boldsymbol{\rho}} - \tilde{\boldsymbol{\rho}} \rangle &= \Gamma_n^\dagger \left[n^{-1} \sum_{i=1}^n \langle \mathbf{X}_i, \mathbf{E}_{x,h}^{\mathbf{X}} \rangle \mathbf{Z}_i^\top n^{1/2} (\boldsymbol{\beta} - \tilde{\boldsymbol{\beta}}) \right] \\ &= \Gamma^{-1} \left[n^{-1} \sum_{i=1}^n \langle \mathbf{X}_i, \mathbf{E}_{x,h}^{\mathbf{X}} \rangle \mathbf{Z}_i^\top n^{1/2} (\boldsymbol{\beta} - \tilde{\boldsymbol{\beta}}) \right] + o_{\mathbb{P}}(1) \\ &= -n^{-1} \sum_{i=1}^n \langle \Gamma^{-1} \mathbf{X}_i, \mathbf{E}_{x,h}^{\mathbf{X}} \rangle \mathbf{Z}_i^\top n^{1/2} (\tilde{\boldsymbol{\beta}} - \boldsymbol{\beta}) + o_{\mathbb{P}}(1) \\ &= \mathbf{E}_{x,h}^{\mathbf{X},\mathbf{Z}} \mathbf{B}^{-1} n^{-1/2} \sum_{i=1}^n \boldsymbol{\eta}_i \varepsilon_i + o_{\mathbb{P}}(1), \end{aligned}$$

where the second equation follows from $\|\Gamma_n^\dagger - \Gamma^\dagger\|_\infty \rightarrow 0$ as well as the construction of Γ^\dagger in Section 2.2. Note that the weak law of large numbers together with Assumption (C3) leads to $-n^{-1} \sum_{i=1}^n \langle \Gamma^{-1} \mathbf{X}_i, \mathbf{E}_{x,\mathbf{h}}^{\mathbf{X}} \rangle \mathbf{Z}_i^\top \xrightarrow{p} \mathbf{E}_{x,\mathbf{h}}^{\mathbf{X},\mathbf{Z}}$. Then we can obtain the last equation using Lemma A.3 and the continuous mapping theorem. ■

Lemma A.8 *Under Assumption (C3),*

$$\sup_{x \in \mathbb{R}} |\bar{\mathbf{Z}}_{x,\mathbf{h}} - \mathbf{E}_{x,\mathbf{h}}^{\mathbf{Z}}| = o_{\mathbb{P}}(1).$$

Proof. It is a straightforward consequence of the weak law of large numbers in \mathcal{H} [see, e.g., Hoffmann-Jørgensen and Pisier (1976)], the continuous mapping theorem, and Assumption (C3). ■

Based on the above lemmas, $T_{n,\mathbf{h}}^4(x) = o_{\mathbb{P}}(1)$. Together with the convergence mode of $T_{n,\mathbf{h}}^2(x)$, we conclude that $T_{n,\mathbf{h}}^1(x)$, $T_{n,\mathbf{h}}^3(x)$ and $T_{n,\mathbf{h}}^5(x)$ are the dominating terms in (14). More specifically, $T_{n,\mathbf{h}}^3(x)$ and $T_{n,\mathbf{h}}^5(x)$ represent the parameter estimation effect that arises due to the estimation of $\boldsymbol{\rho}$ and $\boldsymbol{\beta}$, respectively.

B Proof of theorems

Proof of Theorem 3.1. For any fixed $x \in \mathbb{R}$, Lemmas A.3 to A.8, together with the decompositions (5), (19) and (20), entail that

$$\begin{aligned} T_{n,\mathbf{h}}(x) &= T_{n,\mathbf{h}}^1(x) - T_{n,\mathbf{h}}^3(x) - T_{n,\mathbf{h}}^5(x) + o_{\mathbb{P}}(1) \\ &= n^{-1/2} \sum_{i=1}^n \mathbb{1}_{\{\mathbf{X}_i^{\mathbf{h}} \leq x\}} \varepsilon_i - n^{-1/2} \sum_{i=1}^n \langle \mathbf{E}_{x,\mathbf{h}}^{\mathbf{X}}, \Gamma^\dagger \mathbf{X}_i \rangle \varepsilon_i \\ &\quad - \left(\mathbf{E}_{x,\mathbf{h}}^{\mathbf{Z}} + \mathbf{E}_{x,\mathbf{h}}^{\mathbf{X},\mathbf{Z}} \right) \mathbf{B}^{-1} n^{-1/2} \sum_{i=1}^n \boldsymbol{\eta}_i \varepsilon_i + o_{\mathbb{P}}(1) \\ &= n^{-1/2} \sum_{i=1}^n \{A_x^i - B_x^i - C_x^i\} + o_{\mathbb{P}}(1) \\ &\equiv T_{n0,\mathbf{h}}(x) + o_{\mathbb{P}}(1), \end{aligned}$$

where $A_x^i = \mathbb{1}_{\{\mathbf{X}_i^{\mathbf{h}} \leq x\}} \varepsilon_i$, $B_x^i = \langle \mathbf{E}_{x,\mathbf{h}}^{\mathbf{X}}, \Gamma^\dagger \mathbf{X}_i \rangle \varepsilon_i$ and $C_x^i = \left(\mathbf{E}_{x,\mathbf{h}}^{\mathbf{Z}} + \mathbf{E}_{x,\mathbf{h}}^{\mathbf{X},\mathbf{Z}} \right) \mathbf{B}^{-1} \boldsymbol{\eta}_i \varepsilon_i$. Using Assumption (A2), the central limit theorem, and Slutsky's theorem, $T_{n,\mathbf{h}}(x)$ is asymptotically normal. The joint asymptotic normality of $(T_{n,\mathbf{h}}(x_1), \dots, T_{n,\mathbf{h}}(x_k))$ for $(x_1, \dots, x_k) \in \mathbb{R}^k$ follows by the Cramér-Wold device.

Since \mathbf{X}_i 's, \mathbf{Z}_i 's and ε_i 's are i.i.d. and $\mathbb{E}[\varepsilon | \mathbf{X}, \mathbf{Z}] = 0$ a.s.,

$$\text{Cov} \left[n^{-1/2} \sum_{i=1}^n \{A_s^i - B_s^i - C_s^i\}, n^{-1/2} \sum_{i'=1}^n \{A_t^{i'} - B_t^{i'} - C_t^{i'}\} \right]$$

$$\begin{aligned}
&= \mathbb{E} [A_s^1 A_t^1] - \mathbb{E} [A_s^1 B_t^1] - \mathbb{E} [A_s^1 C_t^1] - \mathbb{E} [B_s^1 A_t^1] + \mathbb{E} [B_s^1 B_t^1] + \mathbb{E} [B_s^1 C_t^1] \\
&\quad - \mathbb{E} [C_s^1 A_t^1] + \mathbb{E} [C_s^1 B_t^1] + \mathbb{E} [C_s^1 C_t^1].
\end{aligned}$$

Applying the tower property with conditioning variables \mathbf{X} and \mathbf{Z} , it follows that

$$\begin{aligned}
\mathbb{E} [A_s^1 A_t^1] &= \int_{\{(\mathbf{x}, \mathbf{z}): \mathbf{x}^h \leq s \wedge t\}} \text{Var} [Y | \mathbf{X} = \mathbf{x}, \mathbf{Z} = \mathbf{z}] dP_{(\mathbf{X}, \mathbf{Z})}(\mathbf{x}, \mathbf{z}), \\
\mathbb{E} [A_s^1 B_t^1] &= \int_{\{(\mathbf{x}, \mathbf{z}): \mathbf{x}^h \leq s\}} \text{Var} [Y | \mathbf{X} = \mathbf{x}, \mathbf{Z} = \mathbf{z}] \langle \mathbf{E}_{t, \mathbf{h}}, \Gamma^\dagger \mathbf{x} \rangle dP_{(\mathbf{X}, \mathbf{Z})}(\mathbf{x}, \mathbf{z}), \\
\mathbb{E} [A_s^1 C_t^1] &= \int_{\{(\mathbf{x}, \mathbf{z}): \mathbf{x}^h \leq s\}} \text{Var} [Y | \mathbf{X} = \mathbf{x}, \mathbf{Z} = \mathbf{z}] \left(\mathbf{E}_{t, \mathbf{h}}^{\mathbf{Z}} + \mathbf{E}_{t, \mathbf{h}}^{\mathbf{X}, \mathbf{Z}} \right) \mathbf{B}^{-1} \boldsymbol{\eta}_1 dP_{(\mathbf{X}, \mathbf{Z})}(\mathbf{x}, \mathbf{z}), \\
\mathbb{E} [B_s^1 B_t^1] &= \int \text{Var} [Y | \mathbf{X} = \mathbf{x}, \mathbf{Z} = \mathbf{z}] \langle \mathbf{E}_{s, \mathbf{h}}, \Gamma^\dagger \mathbf{x} \rangle \langle \mathbf{E}_{t, \mathbf{h}}, \Gamma^\dagger \mathbf{x} \rangle dP_{(\mathbf{X}, \mathbf{Z})}(\mathbf{x}, \mathbf{z}), \\
\mathbb{E} [B_s^1 C_t^1] &= \int \text{Var} [Y | \mathbf{X} = \mathbf{x}, \mathbf{Z} = \mathbf{z}] \langle \mathbf{E}_{s, \mathbf{h}}, \Gamma^\dagger \mathbf{x} \rangle \left(\mathbf{E}_{t, \mathbf{h}}^{\mathbf{Z}} + \mathbf{E}_{t, \mathbf{h}}^{\mathbf{X}, \mathbf{Z}} \right) \mathbf{B}^{-1} \boldsymbol{\eta}_1 dP_{(\mathbf{X}, \mathbf{Z})}(\mathbf{x}, \mathbf{z}), \\
\mathbb{E} [C_s^1 C_t^1] &= \int \text{Var} [Y | \mathbf{X} = \mathbf{x}, \mathbf{Z} = \mathbf{z}] \left(\mathbf{E}_{s, \mathbf{h}}^{\mathbf{Z}} + \mathbf{E}_{s, \mathbf{h}}^{\mathbf{X}, \mathbf{Z}} \right) \mathbf{B}^{-1} \left(\mathbf{E}_{t, \mathbf{h}}^{\mathbf{Z}} + \mathbf{E}_{t, \mathbf{h}}^{\mathbf{X}, \mathbf{Z}} \right)^\top dP_{(\mathbf{X}, \mathbf{Z})}(\mathbf{x}, \mathbf{z}).
\end{aligned}$$

The construction of Γ^\dagger and condition (i) imply that $\|\Gamma^\dagger x - \Gamma^{-1}x\| \xrightarrow{p} 0$, then Cauchy–Schwarz inequality entails that $\mathbb{E} [A_s^1 B_t^1] - C_2(s, t)$, $\mathbb{E} [B_s^1 B_t^1] - C_4(s, t)$ and $\mathbb{E} [B_s^1 C_t^1] - C_5(s, t)$ converge to zero. Applying Slutsky’s theorem, we obtain the finite-dimensional convergence of $T_{n, \mathbf{h}}$.

The tightness of $T_{n, \mathbf{h}}^1$ has been proven in Theorem 1.1 of [Stute \(1997\)](#). For $T_{n, \mathbf{h}}^2$, by Cauchy–Schwarz inequality,

$$\sup_{x \in \mathbb{R}} |T_{n, \mathbf{h}}^2(x)| \leq \sup_{x \in \mathbb{R}} \|\bar{\mathbf{X}}_{x, \mathbf{h}} - \mathbf{E}_{x, \mathbf{h}}^{\mathbf{X}}\| n^{1/2} \|\hat{\boldsymbol{\rho}} - \boldsymbol{\rho}\|,$$

Assumption $\mathbb{E} [\|\hat{\boldsymbol{\rho}} - \boldsymbol{\rho}\|^4] = \mathcal{O}(n^{-2})$ implies that $n^{1/2} \|\hat{\boldsymbol{\rho}} - \boldsymbol{\rho}\| \xrightarrow{p} 0$, while the weak law of large numbers in \mathcal{H} together with Assumption (C3) leads to $\bar{\mathbf{X}}_{x, \mathbf{h}} - \mathbf{E}_{x, \mathbf{h}}^{\mathbf{X}} \xrightarrow{p} 0$ in \mathcal{H} . We finally obtain $\sup_{x \in \mathbb{R}} |T_{n, \mathbf{h}}^2(x)| \xrightarrow{p} 0$ by the continuous mapping theorem.

For the tightness of $T_{n, \mathbf{h}}^3$, define

$$\bar{T}_{n, \mathbf{h}}^3(u) \equiv n^{1/2} \left\langle \mathbb{E} \left[\mathbf{1}_{\{\mathbf{U}^h \leq u\}} \mathbf{X} \right], \hat{\boldsymbol{\rho}} - \boldsymbol{\rho} \right\rangle,$$

with $\mathbf{U}_h = F_h(\mathbf{X}^h)$. Note that

$$T_{n, \mathbf{h}}^3(x) = \bar{T}_{n, \mathbf{h}}^3(F_h(x)).$$

For $0 \leq u_1 < u < u_2 \leq 1$, consider

$$\bar{T}_{n, \mathbf{h}}^3(u) - \bar{T}_{n, \mathbf{h}}^3(u_1) = n^{1/2} \left\langle \mathbb{E} \left[\mathbf{1}_{\{u_1 < \mathbf{U}^h \leq u\}} \mathbf{X} \right], \hat{\boldsymbol{\rho}} - \boldsymbol{\rho} \right\rangle,$$

$$\bar{T}_{n,\mathbf{h}}^3(u_2) - \bar{T}_{n,\mathbf{h}}^3(u) = n^{1/2} \left\langle \mathbb{E} \left[\mathbf{1}_{\{u < \mathbf{U}^{\mathbf{h}} \leq u_2\}} \mathbf{X} \right], \hat{\boldsymbol{\rho}} - \boldsymbol{\rho} \right\rangle.$$

Then, applying Cauchy–Schwarz and Jensen inequalities,

$$\begin{aligned} & \mathbb{E} \left[\left| \bar{T}_{n,\mathbf{h}}^3(u) - \bar{T}_{n,\mathbf{h}}^3(u_1) \right|^2 \left| \bar{T}_{n,\mathbf{h}}^3(u_2) - \bar{T}_{n,\mathbf{h}}^3(u) \right|^2 \right] \\ & \leq n^2 \mathbb{E} \left[\left\| \mathbb{E} \left[\mathbf{1}_{\{u_1 < \mathbf{U}^{\mathbf{h}} \leq u\}} \mathbf{X} \right] \right\|^2 \left\| \mathbb{E} \left[\mathbf{1}_{\{u < \mathbf{U}^{\mathbf{h}} \leq u_2\}} \mathbf{X} \right] \right\|^2 \|\hat{\boldsymbol{\rho}} - \boldsymbol{\rho}\|^4 \right] \\ & = n^2 \mathbb{E} \left[\|\hat{\boldsymbol{\rho}} - \boldsymbol{\rho}\|^4 \int \mathbb{E} \left[\mathbf{1}_{\{u_1 < \mathbf{U}^{\mathbf{h}} \leq u\}} \mathbf{X}(t) \right]^2 dt \int \mathbb{E} \left[\mathbf{1}_{\{u < \mathbf{U}^{\mathbf{h}} \leq u_2\}} \mathbf{X}(t) \right]^2 dt \right] \\ & \leq n^2 \mathbb{E} \left[\|\hat{\boldsymbol{\rho}} - \boldsymbol{\rho}\|^4 \int \mathbb{E} \left[\mathbf{1}_{\{u_1 < \mathbf{U}^{\mathbf{h}} \leq u\}} \mathbf{X}(t)^2 \right] dt \int \mathbb{E} \left[\mathbf{1}_{\{u < \mathbf{U}^{\mathbf{h}} \leq u_2\}} \mathbf{X}(t)^2 \right] dt \right] \\ & = n^2 \mathbb{E} \left[\|\hat{\boldsymbol{\rho}} - \boldsymbol{\rho}\|^4 \right] [F(u) - F(u_1)] [F(u_2) - F(u)] \\ & \leq n^2 \mathbb{E} \left[\|\hat{\boldsymbol{\rho}} - \boldsymbol{\rho}\|^4 \right] [F(u_2) - F(u_1)]^2 \\ & \leq [G(u_2) - G(u_1)]^2, \end{aligned}$$

where $F(u) = \int \mathbb{E} \left[\mathbf{1}_{\{\mathbf{U}^{\mathbf{h}} \leq u\}} \mathbf{X}(t)^2 \right] dt$ and $G(u) = \sup_n \{n^2 \mathbb{E} [\|\hat{\boldsymbol{\rho}} - \boldsymbol{\rho}\|^4]\} F(u)$ are non-decreasing and continuous functions in $[0, 1]$. The weak convergence of $\bar{T}_{n,\mathbf{h}}^3$ in $D([0, 1])$ is obtained by employing Theorem 13.5 in Billingsley (1999) as $\gamma = 2$ and $\alpha = 1$. Then, $T_{n,\mathbf{h}}^3$ converges in \mathcal{H} as a result of the continuous mapping theorem.

Lemma A.2 and Lemma A.8 imply that $T_{n,\mathbf{h}}^4(x) \xrightarrow{p} 0$ uniformly in $x \in \mathbb{R}$. As for $T_{n,\mathbf{h}}^5$, by Assumption (C3), $\mathbf{E}_{x,\mathbf{h}}^{\mathbf{Z}}$ can be regarded as a bounded nonrandom function of $x \in \mathbb{R}$. Together with Lemma A.2, we derive that $T_{n,\mathbf{h}}^5$ weakly converge in \mathcal{H} .

As a consequence of all the above proof, together with Lemma A.1 and Slutsky's theorem, under $H_0^{\mathbf{h}}$, $T_{n,\mathbf{h}}$ weakly converges to a Gaussian process with zero mean and covariance function $K(s, t)$. ■

Proof of Corollary 3.1. The weak convergence of the empirical process $T_{n,\mathbf{h}}(x)$ and the continuous mapping theorem directly lead to that $\|T_{n,\mathbf{h}}\|_{KS} \xrightarrow{\mathcal{L}} \|\mathcal{G}\|_{KS}$.

For the CvM norm, we will prove that $\int_{\mathbb{R}} T_{n,\mathbf{h}}(x)^2 dF_{n,\mathbf{h}}(x) \xrightarrow{\mathcal{L}} \int_{\mathbb{R}} \mathcal{G}(x)^2 dF_{\mathbf{h}}(x)$. The weak law of large numbers in \mathcal{H} and continuous mapping theorem yield that

$$\sup_{x \in \mathbb{R}} |F_{n,\mathbf{h}}(x) - F_{\mathbf{h}}(x)| \xrightarrow{a.s.} 0. \quad (21)$$

It is clear that $\sup_{x \in \mathbb{R}} |T_{n,\mathbf{h}}(x) - \mathcal{G}(x)| \xrightarrow{a.s.} 0$. Note that

$$\begin{aligned} \left| \int_{\mathbb{R}} T_{n,\mathbf{h}}(x)^2 dF_{n,\mathbf{h}}(x) - \int_{\mathbb{R}} \mathcal{G}(x)^2 dF_{\mathbf{h}}(x) \right| & \leq \left| \int_{\mathbb{R}} \{T_{n,\mathbf{h}}(x)^2 - \mathcal{G}(x)^2\} dF_{n,\mathbf{h}}(x) \right| \\ & \quad + \left| \int_{\mathbb{R}} \mathcal{G}(x)^2 \{dF_{n,\mathbf{h}}(x) - dF_{\mathbf{h}}(x)\} \right| \end{aligned}$$

The first term of the right-hand side of the above inequality is $o_{a.s.}(1)$. The trajecto-

ries of the limiting process $\mathcal{G}(x)$ are bounded and continuous almost surely. Applying Helly–Bray Theorem of these trajectories and taking into account (21), one can get $|\int_{\mathbb{R}} \mathcal{G}(x)^2 \{dF_{n,h}(x) - dF_h(x)\}| \xrightarrow{a.s.} 0$. This concludes the proof of Corollary 1. ■

Proof of Theorem 3.2. Under the fixed alternative H_1^h in (9), one has that uniformly in $x \in \mathbb{R}$,

$$\begin{aligned} n^{-1/2}T_{n,h}(x) &= n^{-1} \sum_{i=1}^n \left(Y_i - \mathbf{X}_i^{\rho^*} - \mathbf{Z}_i^{\top} \boldsymbol{\beta} \right) \mathbb{1}_{\{\mathbf{x}_i^h \leq x\}} + n^{-1} \sum_{i=1}^n \langle \mathbf{X}_i, \boldsymbol{\rho}^* - \hat{\boldsymbol{\rho}} \rangle \mathbb{1}_{\{\mathbf{x}_i^h \leq x\}} \\ &\quad + n^{-1} \sum_{i=1}^n \mathbf{Z}_i^{\top} \left(\boldsymbol{\beta} - \tilde{\boldsymbol{\beta}} \right) \mathbb{1}_{\{\mathbf{x}_i^h \leq x\}} \\ &= \mathcal{G}_1(x) + o_{\mathbb{P}}(1), \end{aligned}$$

The first and third terms in the second equation are both Donsker by Corollary 2.10.13 in Vaart and Wellner (1996), thus converging uniformly via the Glivenko–Cantelli theorem. The strong law of large numbers leads to the pointwise convergence of the second term in the second equation for $x \in \mathbb{R}$, while the uniform convergence follows from the Cramér–Wold device and tightness, which can be proved through similar steps in the proof of Theorem 3.1. ■

Proof of Theorem 3.3. Under the sequence of local alternatives H_{1n}^h in (11), one has that uniformly in $x \in \mathbb{R}$,

$$\begin{aligned} T_{n,h}(x) &= n^{-1/2} \sum_{i=1}^n \{ \hat{\varepsilon}_i - n^{-1/2} r(\mathbf{X}_i) \} \mathbb{1}_{\{\mathbf{x}_i^h \leq x\}} + \frac{1}{n} \sum_{i=1}^n r(\mathbf{X}_i) \mathbb{1}_{\{\mathbf{x}_i^h \leq x\}} \\ &= n^{-1/2} \sum_{i=1}^n \left(Y_i - n^{-1/2} r(\mathbf{X}_i) - \mathbf{X}_i^{\hat{\rho}} - \mathbf{Z}_i^{\top} \tilde{\boldsymbol{\beta}} \right) \mathbb{1}_{\{\mathbf{x}_i^h \leq x\}} + \frac{1}{n} \sum_{i=1}^n r(\mathbf{X}_i) \mathbb{1}_{\{\mathbf{x}_i^h \leq x\}} \\ &= n^{-1/2} \sum_{i=1}^n \left(\varepsilon_i^{1n} + \mathbf{X}_i^{\rho_0} + \mathbf{Z}_i^{\top} \boldsymbol{\beta} - \mathbf{X}_i^{\hat{\rho}} - \mathbf{Z}_i^{\top} \tilde{\boldsymbol{\beta}} \right) \mathbb{1}_{\{\mathbf{x}_i^h \leq x\}} + \frac{1}{n} \sum_{i=1}^n r(\mathbf{X}_i) \mathbb{1}_{\{\mathbf{x}_i^h \leq x\}} \\ &= n^{-1} \sum_{i=1}^n (\bar{A}_x^i - \bar{B}_x^i - \bar{C}_x^i) + \frac{1}{n} \sum_{i=1}^n r(\mathbf{X}_i) \mathbb{1}_{\{\mathbf{x}_i^h \leq x\}} + o_{\mathbb{P}}(1) \\ &= n^{-1} \sum_{i=1}^n (\bar{A}_x^i - \bar{B}_x^i - \bar{C}_x^i) + \mathbb{E} \left[r(\mathbf{X}) \mathbb{1}_{\{\mathbf{x}^h \leq x\}} \right] + o_{\mathbb{P}}(1) \\ &\stackrel{\mathcal{L}}{\rightsquigarrow} \mathcal{G}_0(x) + \Delta_r(x), \end{aligned}$$

where $\{\varepsilon_i^{1n}\}$ denoting $\{Y_i - n^{-1/2} r(\mathbf{X}_i) - \mathbf{X}_i^{\rho} - \mathbf{Z}_i^{\top} \boldsymbol{\beta}\}$ are i.i.d. random sequence with mean zero under H_{1n}^h , thus enjoy the same properties as $\{\varepsilon_i\}$ under H_0^h . $\bar{A}_x^i, \bar{B}_x^i, \bar{C}_x^i$ resemble A_x^i, B_x^i, C_x^i defined in the proof of Theorem 3.1, except that $\boldsymbol{\rho}$ under H_0 is replaced by $\boldsymbol{\rho}_0$ under H_{1n}^h . The proof is completed following similar arguments of the proof of Theorem 3.1. ■

Proof of Theorem 4.1. From the simulation process of wild bootstrap, we use

$$\hat{\rho}^* = \Gamma_n^\dagger \Gamma_n \hat{\rho} + (\Gamma_n^\dagger - \Gamma^\dagger) \mathbf{U}_n^* + \Gamma^\dagger \mathbf{U}_n^*$$

to mimic (18). It follows that

$$\hat{\rho}^* - \hat{\rho} = (\Gamma_n^\dagger - \Gamma^\dagger) \mathbf{U}_n^* + \Gamma^\dagger \mathbf{U}_n^*,$$

where $\mathbf{U}_n^* = \frac{1}{n} \sum_{i=1}^n \mathbf{X}_i \otimes U_i^*$.

Similarly, there exists

$$n^{1/2} (\tilde{\beta}^* - \tilde{\beta}) = \left(n^{-1} \tilde{\mathbf{Z}}_b^T \tilde{\mathbf{Z}}_b \right)^{-1} n^{-1/2} (S_{n1} - S_{n2}^* + S_{n3}^*),$$

where S_{n2}^* and S_{n3}^* are same as S_{n2} and S_{n3} with ε_i replaced by U_i^* .

Note that U_i^* 's are independent conditional on $\mathbf{X}_i, \mathbf{Z}_i$ and have identical first and second order moments with ε_i 's, hence the previous proof still holds with ε_i 's replaced by U_i^* 's. Thus uniformly in $x \in \mathbb{R}$,

$$\begin{aligned} T_{n,\mathbf{h}}^*(x) &= n^{-1/2} \sum_{i=1}^n \mathbb{1}_{\{\mathbf{x}_i^{\mathbf{h}} \leq x\}} \left\{ Y_i^* - \mathbf{X}_i^{\hat{\rho}} - \mathbf{Z}^\top \tilde{\beta} \right\} - n^{-1/2} \sum_{i=1}^n \mathbb{1}_{\{\mathbf{x}_i^{\mathbf{h}} \leq x\}} \left\{ \mathbf{X}_i^{\hat{\rho}^* - \hat{\rho}} - \mathbf{Z}^\top (\tilde{\beta}^* - \tilde{\beta}) \right\} \\ &= n^{-1/2} \sum_{i=1}^n \mathbb{1}_{\{\mathbf{x}_i^{\mathbf{h}} \leq x\}} U_i^* - n^{-1/2} \sum_{i=1}^n \langle \mathbf{E}_{x,\mathbf{h}}^{\mathbf{X}}, \Gamma^\dagger \mathbf{X}_i \rangle U_i^* \\ &\quad - \left(\mathbf{E}_{x,\mathbf{h}}^{\mathbf{Z}} + \mathbf{E}_{x,\mathbf{h}}^{\mathbf{X},\mathbf{Z}} \right) \mathbf{B}^{-1} n^{-1/2} \sum_{i=1}^n \boldsymbol{\eta}_i U_i^* + o_{\mathbb{P}}(1) \\ &= T_{n0,\mathbf{h}}^*(x) + o_{\mathbb{P}}(1), \end{aligned}$$

where $T_{n0,\mathbf{h}}^*$ is the wild bootstrap version of $T_{n0,\mathbf{h}}(x)$ with ε_i 's replaced by U_i^* 's. The proof is finished by the similar procedure used in the proof of Theorem 3.1. ■

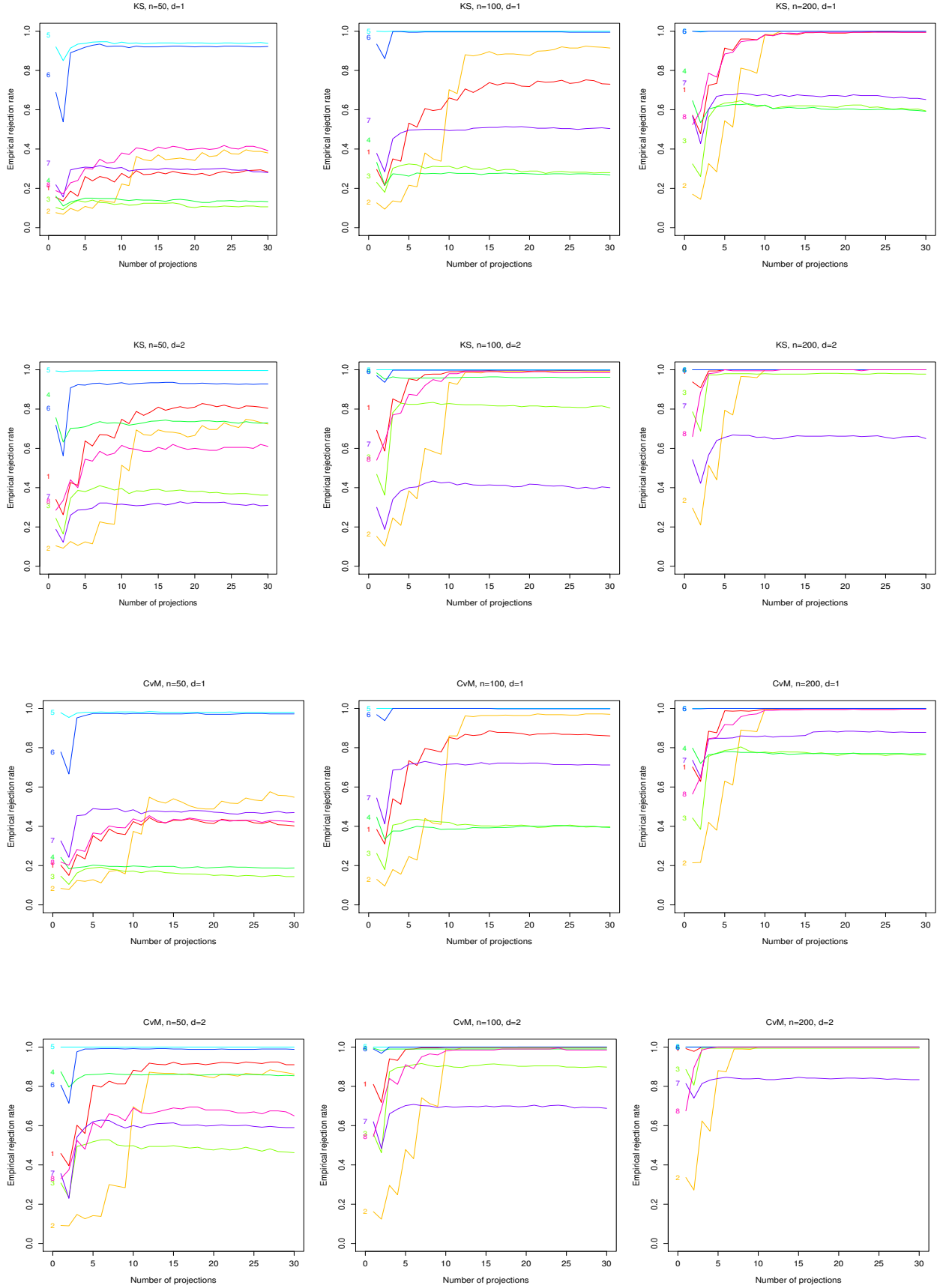


Figure 5: Empirical powers of the CvM and KS tests with the number of projections from 1 to 30 in scenario S_k , $k = 1, \dots, 8$, based on the significance level $\alpha = 0.05$ and the sample sizes $n = 50, 100$, and 200 , respectively. The first and third row correspond to the alternative $H_{k,1}$, while the second and fourth row for $H_{k,2}$, $k = 1, \dots, 8$.

Table 3: Empirical sizes and powers of the CvM and KS tests based on different bandwidth $b = cn^{-1/5}$: left of the parentheses $c = 2$, right of the parentheses $c = 4$; inside the parentheses α is 0.05, with sample size $n = 50, 100, 200$ and the number of projections $K = 7$.

| $H_{k,\delta}$ | $n = 50$ | | | | $n = 100$ | | | | $n = 200$ | | | |
|----------------|---------------|-------|---------------|-------|---------------|-------|---------------|-------|---------------|-------|---------------|-------|
| | CvM | | KS | | CvM | | KS | | CvM | | KS | |
| $H_{1,0}$ | 0.066 (0.056) | 0.056 | 0.058 (0.056) | 0.064 | 0.050 (0.044) | 0.050 | 0.068 (0.062) | 0.044 | 0.038 (0.047) | 0.066 | 0.068 (0.050) | 0.082 |
| $H_{2,0}$ | 0.054 (0.097) | 0.034 | 0.064 (0.090) | 0.050 | 0.052 (0.062) | 0.074 | 0.060 (0.068) | 0.082 | 0.058 (0.060) | 0.068 | 0.056 (0.056) | 0.072 |
| $H_{3,0}$ | 0.050 (0.045) | 0.046 | 0.050 (0.044) | 0.054 | 0.042 (0.048) | 0.064 | 0.044 (0.065) | 0.080 | 0.030 (0.049) | 0.040 | 0.050 (0.054) | 0.038 |
| $H_{4,0}$ | 0.038 (0.050) | 0.042 | 0.044 (0.054) | 0.048 | 0.030 (0.041) | 0.036 | 0.040 (0.039) | 0.036 | 0.036 (0.038) | 0.048 | 0.036 (0.037) | 0.048 |
| $H_{5,0}$ | 0.038 (0.032) | 0.036 | 0.042 (0.040) | 0.032 | 0.030 (0.026) | 0.028 | 0.032 (0.029) | 0.034 | 0.042 (0.043) | 0.040 | 0.042 (0.050) | 0.030 |
| $H_{6,0}$ | 0.040 (0.064) | 0.058 | 0.042 (0.070) | 0.068 | 0.040 (0.049) | 0.042 | 0.046 (0.058) | 0.054 | 0.046 (0.049) | 0.054 | 0.050 (0.051) | 0.046 |
| $H_{7,0}$ | 0.046 (0.036) | 0.038 | 0.052 (0.046) | 0.046 | 0.016 (0.051) | 0.032 | 0.034 (0.060) | 0.046 | 0.028 (0.047) | 0.038 | 0.026 (0.054) | 0.058 |
| $H_{8,0}$ | 0.078 (0.087) | 0.070 | 0.066 (0.095) | 0.080 | 0.082 (0.072) | 0.064 | 0.078 (0.076) | 0.070 | 0.074 (0.055) | 0.066 | 0.068 (0.065) | 0.074 |
| $H_{1,1}$ | 0.284 (0.386) | 0.210 | 0.194 (0.260) | 0.178 | 0.536 (0.796) | 0.516 | 0.412 (0.606) | 0.400 | 0.926 (0.988) | 0.932 | 0.818 (0.960) | 0.804 |
| $H_{2,1}$ | 0.136 (0.170) | 0.120 | 0.120 (0.138) | 0.106 | 0.314 (0.440) | 0.286 | 0.260 (0.380) | 0.252 | 0.688 (0.890) | 0.650 | 0.572 (0.812) | 0.528 |
| $H_{3,1}$ | 0.176 (0.182) | 0.178 | 0.136 (0.128) | 0.142 | 0.370 (0.430) | 0.366 | 0.276 (0.302) | 0.264 | 0.716 (0.804) | 0.718 | 0.580 (0.646) | 0.560 |
| $H_{4,1}$ | 0.230 (0.196) | 0.020 | 0.172 (0.148) | 0.158 | 0.438 (0.396) | 0.444 | 0.312 (0.274) | 0.302 | 0.754 (0.776) | 0.788 | 0.586 (0.626) | 0.598 |
| $H_{5,1}$ | 0.968 (0.980) | 0.986 | 0.918 (0.946) | 0.936 | 1.000 (1.000) | 1.000 | 1.000 (1.000) | 1.000 | 1.000 (1.000) | 1.000 | 1.000 (1.000) | 1.000 |
| $H_{6,1}$ | 0.966 (0.974) | 0.952 | 0.926 (0.934) | 0.890 | 1.000 (1.000) | 0.996 | 0.998 (0.996) | 0.992 | 1.000 (1.000) | 1.000 | 1.000 (1.000) | 1.000 |
| $H_{7,1}$ | 0.446 (0.486) | 0.422 | 0.286 (0.316) | 0.254 | 0.660 (0.730) | 0.678 | 0.450 (0.500) | 0.478 | 0.840 (0.860) | 0.852 | 0.690 (0.684) | 0.678 |
| $H_{8,1}$ | 0.212 (0.402) | 0.204 | 0.204 (0.348) | 0.198 | 0.376 (0.564) | 0.384 | 0.620 (0.492) | 0.352 | 0.668 (0.958) | 0.646 | 0.636 (0.946) | 0.610 |
| $H_{1,2}$ | 0.626 (0.826) | 0.552 | 0.478 (0.670) | 0.394 | 0.970 (0.996) | 0.954 | 0.896 (0.976) | 0.896 | 1.000 (1.000) | 1.000 | 1.000 (1.000) | 0.998 |
| $H_{2,2}$ | 0.180 (0.300) | 0.166 | 0.172 (0.226) | 0.144 | 0.476 (0.742) | 0.490 | 0.406 (0.600) | 0.354 | 0.866 (0.990) | 0.874 | 0.770 (0.966) | 0.774 |
| $H_{3,2}$ | 0.530 (0.528) | 0.526 | 0.378 (0.410) | 0.396 | 0.870 (0.916) | 0.886 | 0.756 (0.830) | 0.748 | 0.998 (0.994) | 0.996 | 0.992 (0.980) | 0.994 |
| $H_{4,2}$ | 0.816 (0.866) | 0.844 | 0.720 (0.736) | 0.702 | 0.986 (0.990) | 0.988 | 0.970 (0.958) | 0.966 | 1.000 (1.000) | 0.998 | 1.000 (1.000) | 0.998 |
| $H_{5,2}$ | 1.000 (1.000) | 1.000 | 0.996 (0.996) | 1.000 | 1.000 (1.000) | 1.000 | 1.000 (1.000) | 1.000 | 1.000 (1.000) | 1.000 | 1.000 (1.000) | 1.000 |
| $H_{6,2}$ | 0.968 (0.992) | 0.972 | 0.922 (0.932) | 0.940 | 0.996 (1.000) | 0.998 | 0.994 (0.998) | 0.998 | 1.000 (1.000) | 1.000 | 1.000 (1.000) | 1.000 |
| $H_{7,2}$ | 0.570 (0.626) | 0.564 | 0.262 (0.322) | 0.304 | 0.742 (0.702) | 0.740 | 0.422 (0.422) | 0.460 | 0.820 (0.842) | 0.836 | 0.610 (0.666) | 0.608 |
| $H_{8,2}$ | 0.468 (0.660) | 0.466 | 0.430 (0.585) | 0.430 | 0.712 (0.950) | 0.716 | 0.672 (0.920) | 0.694 | 0.898 (1.000) | 0.906 | 0.882 (0.995) | 0.892 |

Table 4: Empirical sizes and powers of the CvM and KS tests based on the significant level $\alpha = 0.05$, with sample sizes $n = 50, 100, 200$, the number of projections $K = 7$ and the bandwidth $b = 3n^{-1/5}$.

| $H_{k,\delta}$ | $n = 50$ | | $n = 100$ | | $n = 200$ | |
|----------------|----------|-------|-----------|-------|-----------|-------|
| | CvM | KS | CvM | KS | CvM | KS |
| $H_{1,0}$ | 0.056 | 0.056 | 0.044 | 0.062 | 0.047 | 0.050 |
| $H_{2,0}$ | 0.097 | 0.090 | 0.062 | 0.068 | 0.060 | 0.056 |
| $H_{3,0}$ | 0.045 | 0.044 | 0.048 | 0.065 | 0.049 | 0.054 |
| $H_{4,0}$ | 0.050 | 0.054 | 0.041 | 0.039 | 0.038 | 0.037 |
| $H_{5,0}$ | 0.032 | 0.040 | 0.026 | 0.029 | 0.043 | 0.050 |
| $H_{6,0}$ | 0.064 | 0.070 | 0.049 | 0.058 | 0.049 | 0.051 |
| $H_{7,0}$ | 0.036 | 0.046 | 0.051 | 0.060 | 0.047 | 0.054 |
| $H_{8,0}$ | 0.087 | 0.095 | 0.072 | 0.076 | 0.055 | 0.065 |
| $H_{1,1}$ | 0.386 | 0.260 | 0.796 | 0.606 | 0.988 | 0.960 |
| $H_{2,1}$ | 0.170 | 0.138 | 0.440 | 0.380 | 0.890 | 0.812 |
| $H_{3,1}$ | 0.182 | 0.128 | 0.430 | 0.302 | 0.804 | 0.646 |
| $H_{4,1}$ | 0.196 | 0.148 | 0.396 | 0.274 | 0.776 | 0.626 |
| $H_{5,1}$ | 0.980 | 0.946 | 1.000 | 1.000 | 1.000 | 1.000 |
| $H_{6,1}$ | 0.974 | 0.934 | 1.000 | 0.996 | 1.000 | 1.000 |
| $H_{7,1}$ | 0.486 | 0.316 | 0.730 | 0.500 | 0.860 | 0.684 |
| $H_{8,1}$ | 0.402 | 0.348 | 0.564 | 0.492 | 0.958 | 0.946 |
| $H_{1,2}$ | 0.826 | 0.670 | 0.996 | 0.976 | 1.000 | 1.000 |
| $H_{2,2}$ | 0.300 | 0.226 | 0.742 | 0.600 | 0.990 | 0.966 |
| $H_{3,2}$ | 0.528 | 0.410 | 0.916 | 0.830 | 0.994 | 0.980 |
| $H_{4,2}$ | 0.866 | 0.736 | 0.990 | 0.958 | 1.000 | 1.000 |
| $H_{5,2}$ | 1.000 | 0.996 | 1.000 | 1.000 | 1.000 | 1.000 |
| $H_{6,2}$ | 0.992 | 0.932 | 1.000 | 0.998 | 1.000 | 1.000 |
| $H_{7,2}$ | 0.626 | 0.322 | 0.702 | 0.422 | 0.842 | 0.666 |
| $H_{8,2}$ | 0.660 | 0.585 | 0.950 | 0.920 | 1.000 | 0.995 |

Table 5: The p -value of CvM and KS tests with different numbers of projections in Tecator data set.

| | $K = 2$ | $K = 4$ | $K = 7$ | $K = 10$ | $K = 12$ |
|-----|---------|---------|---------|----------|----------|
| CvM | 0.505 | 0.626 | 0.589 | 0.561 | 0.551 |
| KS | 0.312 | 0.406 | 0.401 | 0.394 | 0.387 |

Table 6: The p -values of the CvM and KS tests with different numbers of projections in the AEMET data set.

| | $K = 2$ | $K = 4$ | $K = 7$ | $K = 10$ | $K = 12$ |
|-----|---------|---------|---------|----------|----------|
| CvM | 0.008 | 0.016 | 0.018 | 0.019 | 0.018 |
| KS | 0.020 | 0.029 | 0.031 | 0.022 | 0.026 |

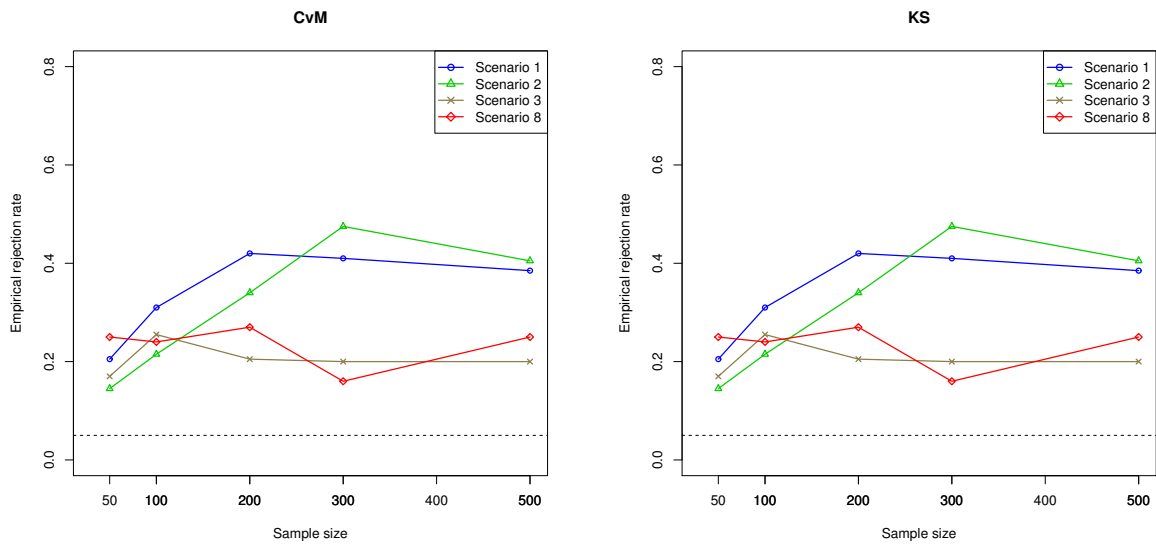


Figure 6: Empirical powers for a Pitman local alternative in scenario S_k , $k = 1, 2, 3, 8$, at the level $\alpha = 0.05$ (dashed line) with the sample sizes $n = 50, 100, 200, 300, 500$.

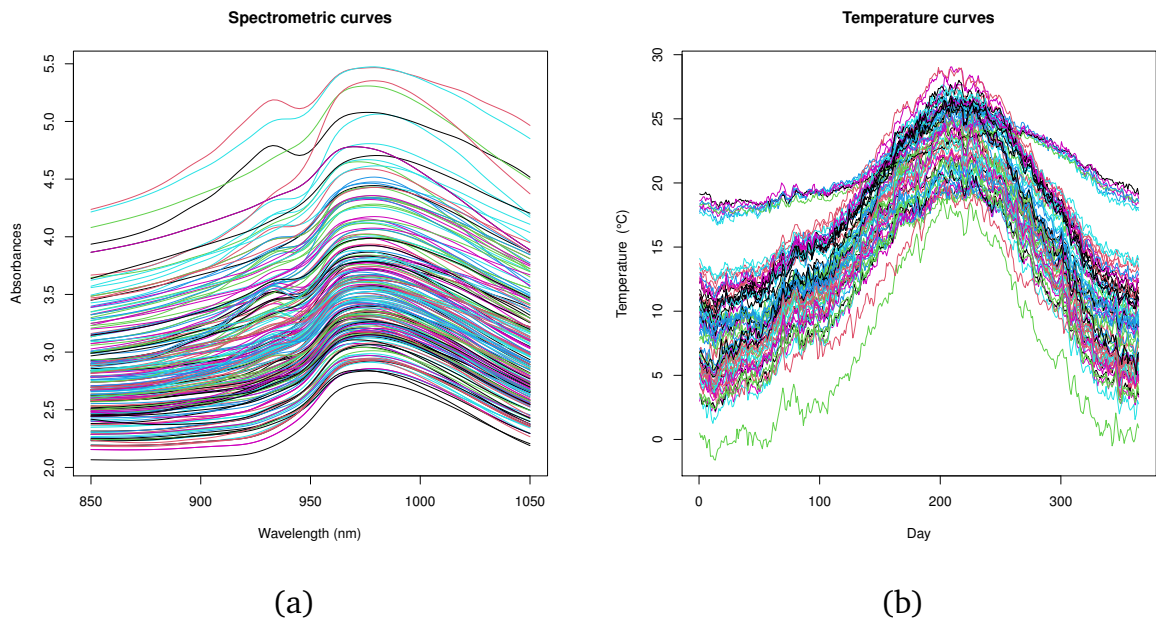


Figure 7: (a) Plot of spectrometric curves in the Tecator data set; (b) Daily mean temperature for the 73 Spanish weather stations.